
TRACE-CLASS GAUSSIAN PRIORS FOR BAYESIAN LEARNING OF NEURAL NETWORKS WITH MCMC

Torben Sell
 School of Mathematics
 University of Edinburgh, UK
 torben.sell@ed.ac.uk

Sumeetpal S. Singh
 Signal Processing and Communications Laboratory
 Department of Engineering
 University of Cambridge, UK
 sss40@cam.ac.uk

November 2, 2021

ABSTRACT

This paper introduces a new neural network based prior for real valued functions on \mathbb{R}^d which, by construction, is more easily and cheaply scaled up in the domain dimension d compared to the usual Karhunen-Loève function space prior. The new prior is a Gaussian neural network prior, where each weight and bias has an independent Gaussian prior, but with the key difference that the variances decrease in the width of the network in such a way that the resulting function is *almost surely* well defined in the limit of an infinite width network. We show that in a Bayesian treatment of inferring unknown functions, the induced posterior over functions is amenable to Monte Carlo sampling using Hilbert space Markov chain Monte Carlo (MCMC) methods. This type of MCMC is popular, e.g. in the Bayesian Inverse Problems literature, because it is stable under *mesh refinement*, i.e. the acceptance probability does not shrink to 0 as more parameters of the function's prior are introduced, even *ad infinitum*. In numerical examples we demonstrate these stated competitive advantages over other function space priors. We also implement examples in Bayesian Reinforcement Learning to automate tasks from data and demonstrate, for the first time, stability of MCMC to mesh refinement for these type of problems.

Keywords Bayesian Neural Networks · Value Function Estimation · preconditioned Crank Nicolson · Langevin Dynamics · Bayesian Reinforcement Learning

1 Introduction

Generating samples from probability measures on function spaces is both a challenging computational problem and a very useful tool for many applications, including mathematical modelling in bioinformatics [Quarteroni et al., 2017], data assimilation in reservoir models [Iglesias et al., 2013], and velocity field estimation in glaciology [Minchew et al., 2015], amongst many others. This paper addresses the problem of defining a computationally and statistically favourable function space prior.

In Bayesian inference on separable Hilbert spaces [Stuart, 2010], many posterior measures π are absolutely continuous with respect to their prior μ_0 (often a Gaussian measure, see Knapik et al. [2011] and Dashti et al. [2013], but not always, see Dashti et al. [2011], Hosseini [2017], and Hosseini and Nigam [2017]), with the likelihood acting as the Radon-Nikodym derivative $d\mu/d\mu_0 \propto \mathcal{L}$. Samples from a Gaussian prior on a separable Hilbert space have a convenient expansion as the sum of the product of independent Gaussian random variables with the countable basis (see (1)) which is known as the Karhunen-Loève (KL) expansion. These posteriors come with a variety of theoretical results, such as concentration inequalities and contraction rates, see e.g. Agapiou et al. [2013], Nickl and Giordano [2020], Knapik et al. [2011], van der Vaart et al. [2008]. Truncating the KL expansion then reduces the problem of sampling from infinite-dimensional measures to sampling from a finite-dimensional parameter space. This truncated approximation to the true posterior gets better by including more terms of the expansion. The practical applicability of these priors are, however, restricted to inferring unknown functions with low-dimensional domain, as the orthogonal basis required for the KL expansion results in the complexity scaling exponential with the dimension of the unknown function's domain. Another approach to define function space priors are Bayesian Neural Networks (BNNs) [Neal, 1995, 2012] which currently enjoy a resurgence of interest in the machine learning community. A BNN is a random function obtained by

placing a prior distribution over the weights and biases of a neural network, with the default choice being a centered Gaussian prior on the weights with variances that scale as $\mathcal{O}(1/N^{(l)})$, where $N^{(l)}$ is the number of nodes in layer l . Some authors argue for heavy-tailed priors on the parameters which has been initially investigated in Neal [1995]. Although some theoretical results exist [Matthews et al., 2018], popular criticisms include the lack of interpretability of the resulting BNNs, and recent work [Wenzel et al., 2020] has highlighted inter alia that novel priors are needed. Sampling approaches include Hamiltonian Monte Carlo [Neal, 1995], and more advanced integrators [Leimkuhler et al., 2019]. However, inference is often limited to finding the maximum-a-posteriori (MAP) estimate of the posterior [Welling and Teh, 2011], and the $\mathcal{O}(1/N^{(l)})$ scaling implies one cannot easily add nodes to a layer to obtain more accurate estimates: one would either have to adjust the prior variances for all nodes within the amended layer, thereby changing the prior, or not adjust the prior resulting in exploding functions [Matthews et al., 2018]. Other function space priors include Deep Neural Networks and Deep Gaussian Processes [Damianou and Lawrence, 2013, Dunlop et al., 2018], and in Dunlop et al. [2018] inference is done using similar function space MCMC techniques to the ones we employ.

To calculate expectations with respect to the Bayesian posterior of the unknown function, computational methods are required as the relevant integrals are usually not analytically tractable. Two popular sampling algorithms for posteriors defined on Hilbert spaces are the preconditioned Crank-Nicolson (pCN) algorithm and its likelihood-informed counterpart the preconditioned Crank-Nicolson Langevin (pCNL) algorithm, which arise from clever (and in a way optimal) discretisations of certain stochastic differential equations [Cotter et al., 2013]. These samplers are asymptotically exact and have a dimension-independent mixing rate in the sense that their proposal ‘step size’ does not depend on the number of terms in the KL truncation [Hairer et al., 2014, Eberle et al., 2014]. This stands in stark contrast to the well-known dimensional-dependent scaling of popular MCMC algorithms such as Random Walk Metropolis and Metropolis Adjusted Langevin Algorithm [Roberts and Rosenthal, 1998, Roberts et al., 2001]. Geometric [Beskos et al., 2017] and likelihood-informed [Cui et al., 2016] modifications of pCN can reduce the computational cost provided one knows which basis functions are informed by the data, but they cannot circumvent the costly scaling in the domain dimension. This is presumably one reason why these methods have rarely been used for inferring unknown functions with domains larger than dimension two (i.e. \mathbb{R}^2) in reported examples in the literature.

This paper introduces a new neural network based prior, coined *trace-class* neural network priors, which allows for scalable (in the domain dimension) Bayesian function space inference. Hilbert space MCMC algorithms are then used to sample from the resulting posteriors, and owing to their stability under mesh-refinement, enhances the practical utility of our framework. In addition to comparisons with reported examples in the literature, we also demonstrate our technique’s usefulness on a challenging 17-dimensional Bayesian Reinforcement learning example where the aim is to learn the *value function* (a function on \mathbb{R}^{17}) that can automate a task demonstrated by an expert – we combine the noisy expert data with a trace-class NN prior to yield a Bayesian formulation.

The main contributions of this paper are as follows:

- We introduce a new *trace-class* Gaussian prior for neural networks, which is both well defined for infinite width NNs and has a degree of smoothness, and demonstrate its practical utility. The prior is independent, centred, and Gaussian across the NN’s weights and biases but is non-exchangeable over the weights within each layer and has a summable variance sequence. The latter, which gives it the trace-class property, ensures it is a valid prior for an infinite width network, while the former results in parameters being better identified from an inference perspective. We further show that this prior is appropriate for use with Hilbert space MCMC methods (Theorem 1). The practical implications of this is that it is valid for the infinite-width limit of the NN and not just finite-dimensional projections of it (e.g. like the Random Walk Metropolis-Hastings algorithm), enjoys a dimension-independent mixing rate and, owing to the inherent scalability of neural networks to its number of inputs, is suitable for applications with high-dimensional state spaces.
- We propose a suitable likelihood for Bayesian Reinforcement Learning (BRL) for inferring the unknown continuous state value function that best describes an observed state-action data sequence. Theorem 2 and Lemma 1 justify the use of this likelihood with Gaussian prior measures on function spaces, and with our proposed neural network prior. This likelihood is also potentially of interest to the machine learning community in its own right.
- We apply Hilbert space MCMC methods to infer the unknown optimal value function in two continuous state control problems, using both our new prior and likelihood function. These exercises motivate the need for NN function priors that are, unlike a canonical orthogonal basis prior for that domain, scalable in the domain dimension, and for the first time demonstrates dimension-independent mixing of MCMC for Bayesian Inverse Reinforcement Learning.

The rest of this paper is organised as follows: In Section 2 we introduce the general inference problem, describe the canonical orthogonal basis for functions on \mathbb{R}^d , describe MCMC methods on an infinite-dimensional Hilbert space including their construction and the assumptions under which these methods are well-defined. Section 3 introduces the trace-class neural network prior and states one of our main theoretical results, showing that the proposed prior satisfies

the necessary assumptions to be used with a Hilbert space MCMC algorithm. In Section 4 we state the Bayesian Reinforcement Learning (BRL) problem and introduce the likelihood to be used for inferring continuous state value functions from state-action data. We then show that the likelihood satisfies the assumptions needed to be admissible in a Hilbert space MCMC setting. Finally, Section 5 provides numerical results for the proposed prior and the likelihood for different control problems. Proofs can be found in the appendix.

1.1 Notation

We use curly letters (\mathcal{X} and \mathcal{A}) for spaces and sets. Subscripts denote both time and spatial variables, but it will be clear from the context which ones we are considering. Value functions are denoted with the letter v throughout, and in Section 2.2 we follow the notation introduced by Cotter et al. [2013]. Φ denotes the Gaussian cumulative distribution function (cdf), ϕ the Gaussian probability density function (pdf). φ is used for basis functions, ζ denotes an activation function. The likelihood function we will write as \mathcal{L} , the log-likelihood as ℓ , and T is the number of data points used in the likelihood. ℓ^2 also denotes the space of square-summable sequences, and further the space of square-integrable functions, with respect to the Lebesgue measure, from $\mathcal{X} \subseteq \mathbb{R}^d$ to \mathbb{R} is denoted $L^2(\mathcal{X}, \mathbb{R})$ or simply L^2 . \mathcal{T} denotes the deterministic state dynamics, mapping a state-action pair (x, a) to the next state x' .

2 Problem Formulation

The objective is to sample from a target distribution μ defined over an infinite-dimensional separable Hilbert space. The targets of interest in this work are Bayesian posterior distributions arising from a Gaussian prior measure μ_0 and a likelihood which can be evaluated point wise. One such likelihood is the Gaussian likelihood that arises from observations of a solution to a PDE with additive Gaussian noise given in Section 3.3, which is a standard likelihood in the Bayesian Inverse problems literature [Stuart, 2010]. The other likelihood we will work with is one for continuous state control problems which is introduced in Section 4. In what follows, we will assume that the posterior has a density with respect to the prior, in which case the Radon-Nikodym derivative is well defined and is proportional to the likelihood. The posterior density with respect to the prior is given by $\frac{d\mu}{d\mu_0}(u) = \frac{1}{Z} \exp(\ell(y|u))$, where y are observations, ℓ is the log-likelihood, and $Z = \int \exp(\ell(y|u))\mu_0(du)$ is the normalisation constant.

For an infinite-dimensional separable Hilbert space \mathcal{H} , say $\mathcal{H} = L^2(\mathcal{X}, \mathbb{R})$ to frame the discussion in this section (and later in Section 3 the sequence space $\mathcal{H} = \ell^2$), there exists an orthonormal basis $\{\varphi_i\}_{i=1}^{\infty}$ such that any element $u \in \mathcal{H}$ can be obtained as the limit $u(x) = \lim_{N \rightarrow \infty} \sum_{i=1}^N a_i \varphi_i(x)$, where $a_i = \langle u, \varphi_i \rangle_{\mathcal{H}}$ with $\langle u, \varphi_i \rangle_{\mathcal{H}}$ denoting the inner product on \mathcal{H} . Let the prior $\mu_0 = \mathcal{N}(0, \mathcal{C})$ be a Gaussian measure on \mathcal{H} . If the operator \mathcal{C} is trace-class with orthonormal eigenvalue-eigenfunction pairs $(\lambda_i^2, \varphi_i(x))$, $i = 1, 2, \dots$, one can sample from μ_0 by sampling a sequence of $\xi_i \sim \mathcal{N}(0, \lambda_i^2)$ and by then defining

$$u(x) = \sum_{i=1}^{\infty} \xi_i \varphi_i(x). \quad (1)$$

The sum defines $u(x) \in \mathcal{H}$ almost surely and is the Karhunen-Loève (KL) expansion [Giné and Nickl, 2016]. One may thus think of a sample from the Gaussian measure as the sum of a sequence of 1-dimensional Gaussians with summable variances. This allows us to truncate the series expansion such that we have N active terms, with the remainder, or approximation error, tending to zero as N increases:

$$u(x) = \sum_{i=1}^N \xi_i \varphi_i(x) + \sum_{i=N+1}^{\infty} \xi_i \varphi_i(x), \quad \|u(x) - \sum_{i=1}^N \xi_i \varphi_i(x)\|^2 = \sum_{i=N+1}^{\infty} \|\xi_i \varphi_i(x)\|^2 = \sum_{i=N+1}^{\infty} \xi_i^2 < \infty \quad \text{a.s.}$$

Other more elaborate truncation schemes are discussed in Cotter et al. [2013], but we will focus on a fixed number of terms for computational and notational convenience. For some applications, φ_i for large i can be interpreted as high-oscillating functions which may not be discernible by the observation operator, see the example in Section 3.3 or Figure 1, where the large i coefficients are responsible for the oscillating function in the left panel, and forced to 0 on the right. Note that, given some $u \in \mathcal{H}$, we can let u' be u with i -th component set to 0, i.e. $u' = u - \langle u, \varphi_i \rangle \varphi_i$. It follows from Assumption 4 that $\lim_{i \rightarrow \infty} \ell(y|u') = \ell(y|u)$, for any $u \in \mathcal{H}$. Following the approach of [Stuart, 2010, Theorem 4.6] this closeness of the likelihoods $\ell(y|u)$ and $\ell(y|u - \langle u, \varphi_i \rangle \varphi_i)$ translates to closeness of the corresponding posteriors.

We emphasise that the above discussion holds not only for the space $\mathcal{H} = L^2(\mathcal{X}, \mathbb{R})$, which is predominantly how it is applied in Beskos et al. [2008], Cotter et al. [2013], Beskos et al. [2017], but also for $\mathcal{H} = \ell^2$ (with the only change being the choice of the orthonormal basis), which will be of particular importance in this paper. In infinite-dimensional spaces, one has to be careful to ensure the posterior is well defined, see Stuart [2010] for a discussion on Gaussian priors and likelihoods given through possibly non-linear mappings, observed in Gaussian noise. We will work with the following assumptions, which we prove are satisfied for the likelihood defined in Section 4.

1. μ_0 is a Gaussian prior defined on a separable Hilbert space \mathcal{H} , with a trace-class covariance operator \mathcal{C} , that is, the eigenvalues λ_i^2 corresponding to the eigenfunctions φ_i satisfy $\sum_i \lambda_i^2 < \infty$;
2. The posterior is well-defined, i.e. the integral of the likelihood with respect to the prior is positive and finite.

2.1 A canonical approximation for functions on \mathbb{R}^d

Consider a d -dimensional hypercube $\mathcal{X} = [0, 1]^d$, the Hilbert space $\mathcal{H} = L^2(\mathcal{X}, \mathbb{R})$, and a Gaussian prior measure μ_0 on \mathcal{H} . A Bayesian approach entails choosing the covariance matrix \mathcal{C} for the Gaussian prior μ_0 , and we discuss a canonical choice below. If the problem requires it, as in Section 3.3 where a PDE is solved, it is possible to choose \mathcal{C} such that the samples are almost surely differentiable.

One problem with this approach is that it scales badly with dimension: say one has eigenvalues λ_i and basis functions φ_i for a 1-dimensional function, and truncates the KL expansion (1) after N terms. The easiest way to scale this basis up to a d -dimensional domain is by taking a tensor product of the basis, see e.g. Iserles and Nørsett [2009] for the multivariate Fourier basis, or Wojtaszczyk [1997] for Wavelets and other basis expansions. For the KL expansion, we thus get, for a multi-index $k = (k_1, \dots, k_d)$ with $k_i = 1, \dots, N$,

$$u(x) = \sum_k \xi_k \varphi_k(x) = \sum_{k_1=1}^N \cdots \sum_{k_d=1}^N \left[\xi_{k_1, \dots, k_d} \prod_{j=1}^d \varphi_{k_j}(x_j) \right], \quad (2)$$

where $\xi_{k_1, \dots, k_d} \sim \mathcal{N}(0, \lambda_{k_1, \dots, k_d}^2)$ with $\lambda_{k_1, \dots, k_d}$ being a function of the respective eigenvalues λ_{k_i} capturing the correlation between dimensions. In total, there are N^d active terms, that is, the complexity is exponential in the dimension d . This will be computationally prohibitively expensive, even for moderately small d .

To circumvent the exponential cost in the domain dimension, one may want to exploit any knowledge of independence that one knows of. Assume, for example, that the function of interest can be approximated as $u(x) \approx v_0 + \sum_{i=1}^d u_i(x_i)$ with $u_i : [0, 1] \rightarrow \mathbb{R}$, $\int u_i(x_i) dx_i = 0$. With this approximation, the number of terms to be inferred is linear in d . In practice, this is often oversimplifying. More generally, one can use approximations including higher order functions following Sobol [1993], e.g.

$$u(x) \approx \sum_{i=1}^d u_i(x_i) + \sum_{i=1}^d \sum_{j=i+1}^d u_{i,j}(x_i, x_j), \quad (3)$$

with $dN + \frac{d(d-1)}{2}N^2$ coefficients to be estimated. Using such an approximation can achieve a massive dimension reduction, avoiding the inference of all N^d coefficients, but requires good knowledge of the properties of the quantities of interest. With the approximation (3) in mind, one restricts oneself to the prior on finitely many random functions u_i and $u_{i,j}$, each of which themselves is sampled from a Gaussian measure $\mathcal{N}(0, \mathcal{C}_1)$, or $\mathcal{N}(0, \mathcal{C}_2)$, respectively. One identifies each of these functions with their Karhunen-Loève expansion

$$u_i(x_i) = \sum_{k=1}^{\infty} \xi_{i,k} \varphi_k(x_i), \quad u_{i,j}(x_i, x_j) = \sum_{k=1}^{\infty} \xi_{i,j,k} \psi_k(x_i, x_j) \quad (4)$$

where the φ_k and ψ_k are the eigenfunctions corresponding to the eigenvalues $\lambda_{\varphi,k}^2$ and $\lambda_{\psi,k}^2$, respectively. The $\xi_{i,k}$ and $\xi_{i,j,k}$ are independent normal random variables $\xi_{i,k} \sim \mathcal{N}(0, \lambda_{\varphi,k}^2)$ and $\xi_{i,j,k} \sim \mathcal{N}(0, \lambda_{\psi,k}^2)$. As before one requires the covariance operators to be *trace-class*, and truncates the expansion (4) after a finite number of term.

The numerical experiments using the KL function space prior in this paper are based on the following Fourier basis functions, φ_k defined on $[0, 1]$, $\psi_k = \psi_{k_1, k_2}$ defined on $[0, 1]^2$ and indexed by a double index $k = (k_1, k_2) \in \mathbb{N} \times \mathbb{N}$:

$$\begin{aligned} \varphi_{2k}(x_i) &= \sin(\pi k x_i) \\ \varphi_{2k+1}(x_i) &= \cos(\pi k x_i) \\ \psi_{2k_1, 2k_2}(x_i, x_j) &= \varphi_{2k_1}(x_i) \varphi_{2k_2}(x_j) = \sin(\pi k_1 x_i) \sin(\pi k_2 x_j) \\ \psi_{2k_1+1, 2k_2}(x_i, x_j) &= \varphi_{2k_1+1}(x_i) \varphi_{2k_2}(x_j) = \cos(\pi k_1 x_i) \sin(\pi k_2 x_j) \\ \psi_{2k_1, 2k_2+1}(x_i, x_j) &= \varphi_{2k_1}(x_i) \varphi_{2k_2+1}(x_j) = \sin(\pi k_1 x_i) \cos(\pi k_2 x_j) \\ \psi_{2k_1+1, 2k_2+1}(x_i, x_j) &= \varphi_{2k_1+1}(x_i) \varphi_{2k_2+1}(x_j) = \cos(\pi k_1 x_i) \cos(\pi k_2 x_j), \end{aligned} \quad (5)$$

for $i \neq j$, with corresponding eigenvalues

$$\lambda_{\varphi, 2k}^2 = \lambda_{\varphi, 2k+1}^2 = \frac{1}{k^\alpha}, \quad \lambda_{\psi, 2k_1, 2k_2}^2 = \lambda_{\psi, 2k_1+1, 2k_2}^2 = \lambda_{\psi, 2k_1, 2k_2+1}^2 = \lambda_{\psi, 2k_1+1, 2k_2+1}^2 = \frac{1}{(\sqrt{k_1^2 + k_2^2})^\alpha}. \quad (6)$$

See Figure 1 for some representative draws from this prior, which is a modification from the prior used in Section 4.2 of Beskos et al. (2017). The covariance operator is of the form $-\Delta^{-\alpha}$ where Δ denotes the Laplacian, and we allow both Dirichlet (e.g. $\varphi_{2k}(0) = \varphi_{2k}(1) = 0$) and Neumann boundary conditions (e.g. $\varphi'_{2k+1}(0) = \varphi'_{2k+1}(1) = 0$), with opposing sides of the square $[0, 1]^2$ satisfying the same boundary conditions.

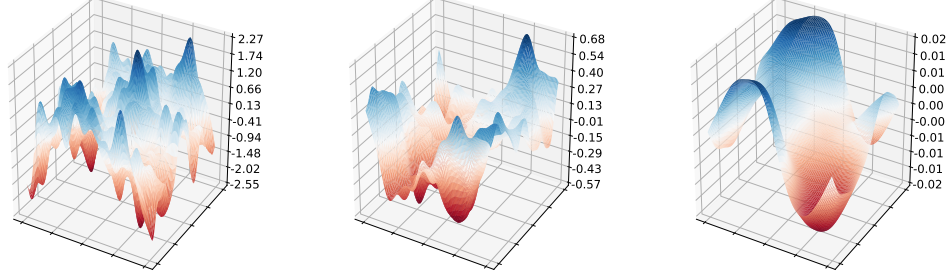


Figure 1: Three samples from the Karhunen-Loève prior; the basis functions are the two-dimensional Fourier functions. In ascending order from left to right we set $\alpha \in \{1.001, 1.5, 3\}$ with the eigenvalues scaling as $\lambda_k^2 \propto 1/(k_1^2 + k_2^2)^\alpha$, for the double index $k = (k_1, k_2)$. The tuning parameter α controls the smoothness of the samples.

Approximations such as (3) are likely to be overly restrictive and if not would still require a good understanding of the functions of interest, which is generally overly restrictive: the statistician or researcher needs to have a good understanding about which coefficients of the eigen expansion are informed by the likelihood, and should therefore be included in the analysis. Section 3 will introduce a prior which scales favourably with the domain-dimension as it does not require pre-defining an orthogonal basis.

2.2 Metropolis-Hastings algorithms on Hilbert spaces

This section recapitulates how to define ‘sensible’ Metropolis-Hastings Markov chain Monte Carlo algorithms for inference over the ξ_i in (1). The use of Markov chains is a popular approach to sample from distributions on finite-dimensional state spaces (see Brooks et al. [2011] for an overview of MCMC methods). Here, we review algorithms which can theoretically deal with arbitrarily many basis coefficients, without the usual problem of the acceptance probability degenerating as one includes more coefficients. This property, known as *stability under mesh-refinement*, is not satisfied by the popular Random Walk Metropolis algorithm (RWMH, Hastings [1970]), or by the Metropolis Adjusted Langevin Algorithm (MALA, Roberts et al. [1996]).

Two algorithms which are both dimension-independent are the preconditioned Crank-Nicolson (pCN) and the preconditioned Crank-Nicolson Langevin (pCNL) algorithms, the former introduced as early as Neal [1998] and both derived and discussed in Cotter et al. [2013]. Motivated by the idea of increasing dimensions translating to evaluating a function on a finer mesh, we refer to the dimension-independence of these algorithms as *stability under mesh-refinement*. Both algorithms can be seen as a discretisation of the following stochastic partial differential equation:

$$\frac{du}{ds} = -\mathcal{K}(C^{-1}u - \gamma D\ell(u)) + \sqrt{2\mathcal{K}} \frac{dB}{ds}, \quad (7)$$

where $D\ell$ is the Fréchet derivative of the log-likelihood¹, \mathcal{K} is a preconditioner, C is the covariance operator of the Gaussian prior measure, B is a Brownian motion, and γ a tuning parameter: if $\gamma = 0$, the invariant distribution of (7) is the prior μ_0 , and for $\gamma = 1$ the invariant distribution is the posterior μ . With the choice $\mathcal{K} = C$ (the preconditioned case, such that the dynamics are scaled to the prior variances), discretising (7) using a Crank-Nicolson scheme results in pCN (for $\gamma = 0$) and pCNL (for $\gamma = 1$). The resulting discretisations can be simplified to

$$v = \sqrt{1 - \beta^2}u + \beta w, \quad w \sim \mathcal{N}(0, C), \quad (\text{pCN}) \quad (8)$$

$$v = \frac{1}{2 + \delta} \left[(2 - \delta)u + 2\delta C D\ell(u) + \sqrt{8\delta}w \right], \quad w \sim \mathcal{N}(0, C), \quad (\text{pCNL}) \quad (9)$$

for step sizes $\beta \in (0, 1]$ and $\delta \in (0, 2)$, respectively. Note that due to the discretisation scheme used, pCN is prior-reversible, and using it as a proposal in a Metropolis-Hastings sampler to target the posterior, the proposal is accepted

¹Note that we use the log-likelihood ℓ rather than the potential $\Phi = -\ell$ as the authors of Cotter et al. [2013].

with probability $\min\{1, \exp(-\ell(u) + \ell(v))\}$. If the pCNL dynamics are used as a proposal for a MH scheme, the acceptance probability is given by $\min\{1, \exp(\rho(u, v) - \rho(v, u))\}$ where

$$\rho(u, v) = -\ell(u) - \frac{1}{2}\langle v - u, \mathcal{D}\ell(u) \rangle - \frac{\delta}{4}\langle u + v, \mathcal{D}\ell(u) \rangle + \frac{\delta}{4}\|\sqrt{C}\mathcal{D}\ell(u)\|^2.$$

Both pCN and pCNL are such that, for an uninformative likelihood, all moves are accepted. In practice, the likelihood Assumptions 3 and 4 ensure that, unlike RWMH or MALA, neither pCN nor pCNL require their step size β or δ to go to 0 as one includes more coefficients in the KL expansions [Cotter et al., 2013].

For mathematical completeness, we emphasise that in order to ensure that the processes arising from the above defined transition kernels have the desired stationary distribution, one needs to check that they yield a strong aperiodic, recurrent Harris chain (giving the existence of a unique stationary distribution Athreya and Ney [1978]), and satisfy the detailed balance condition (showing that the stationary distribution is the one of interest Tierney et al. [1998]).

To conclude this section, we state the assumptions [Cotter et al., 2013, Assumptions 6.1] under which both pCN [Cotter et al., 2013, Thm 6.2] and pCNL (see Theorem 4 in the appendix) are well defined, where Assumption 5 is only required for pCNL [Beskos et al., 2017]:

3. There exist constants $K > 0, p > 0$ such that $0 \leq -\ell(y|u) < K(1 + \|u\|^p)$ holds for all $u \in \mathcal{H}$;
4. $\forall r > 0 \exists K(r) > 0$ such that for all u, v with $\max(\|u\|, \|v\|) < r$, we have $|\ell(y|u) - \ell(y|v)| \leq K(r)\|u - v\|$;
5. $\forall u \in \mathcal{H}: \mathcal{C}\mathcal{D}\ell(u) \in \text{Im}(\mathcal{C}^{1/2})$, μ_0 -almost surely. That is, for any draw u from the prior, the *preconditioned* differential operator at u is in the Cameron-Martin space of the prior with probability 1.

3 Trace-Class Neural Network Priors

The Gaussian prior on $\mathcal{H} = L^2(\mathcal{X}, \mathbb{R})$ exploits the isometry between the function space $L^2(\mathcal{X}, \mathbb{R})$ and the sequence space ℓ^2 using the Karhunen-Loève expansion [Giné and Nickl, 2016], but the computational complexity of using a basis-expansion on a high-dimensional domain is unfeasible even when using approximate function representations such as in Sobol [1993].

Neural networks have shown excellent empirical performance in high-dimensional function regression tasks, and Bayesian neural networks (BNNs) use their architecture to define priors over such functions. BNNs are popular as they empirically show good results, and scale well with the dimension of the domain. While some theoretical results about their approximation ability and infinite-width behaviour are known [Hornik, 1991, Matthews et al., 2018], the interpretability of the posteriors arising from Bayesian neural networks are limited, and priors are often understood as a regularisation method in optimisation [Welling and Teh, 2011], rather than the actual prior belief one has on the weights; see also Lipton [2018] for a broader discussion of interpretability.

We now propose a prior for the parameters that define a neural network which, in contrast to existing priors for neural networks, generate almost surely well-defined functions for an infinite-width neural network. This is achieved by parameterising the infinite width neural network using sequences in the Hilbert space $\mathcal{H} = \ell^2$, the space of square-summable real valued sequences, and endow it with a trace-class Gaussian prior. This would then allow inference for such neural networks to be conducted using the dimension-independent MCMC methods discussed in Section 2.2.

Through the architecture of the neural network, the prior μ_0 over the parameters implicitly defines a prior on the output function of the neural network. Under mild assumptions on the network architecture, and if \mathcal{X} is compact, the output functions v_θ are μ_0 -almost surely square-integrable over \mathcal{X} , and the prior thus naturally defines a prior over $L^2(\mathcal{X}, \mathbb{R})$ as well. The proposed prior is also more flexible than the Karhunen-Loève expansion of a Gaussian measure: one neither needs to specify a covariance operator and find its eigenfunctions, nor decide on a basis which is then used to define a Gaussian prior. By giving up the orthogonality of these eigenfunctions which allow for a rich theoretical analysis, one gains on the performance side. We coin the term *trace-class neural network prior* (tcNN) to emphasise that the prior leads to a well-defined function space prior if the variances of all parameters are appropriately summable. The term is well-established for Gaussian measures, where these are called trace-class if the eigenvalues of the covariance operator are summable.

Consider a n -layer feed-forward fully-connected neural network illustrated in Figure 2. The width of layer l is N^l , the input to the first layer is $x \in [0, 1]^d$, the domain of the function to be approximated, and let $v(x) = f_1^{(n+1)}(x) \in \mathbb{R}$ denote the network's output; for notational convenience we write $N^0 = d$ and $N^{n+1} = 1$. The network is described fully by the following set of real valued weights and biases,

$$w = \left\{ w_{i,j}^{(l)} \right\}_{i=1, j=1, l=1}^{N^l, N^{l-1}, n+1}, \quad b = \left\{ b_i^{(l)} \right\}_{i=1, l=1}^{N^l, n+1}, \quad \theta = (w, b), \quad (10)$$

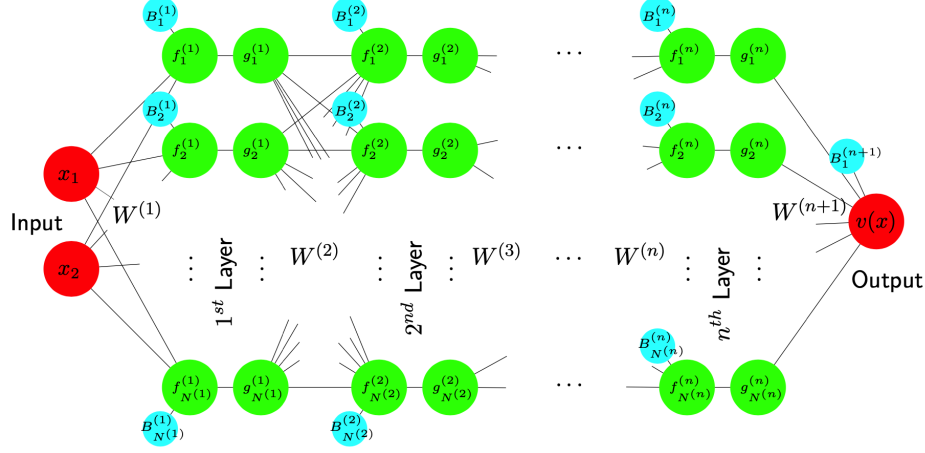


Figure 2: A n -layer feed-forward neural network defining a function $v : \mathbb{R}^2 \rightarrow \mathbb{R}$. Note that $g_i^{(l)} = \zeta(f_i^{(l)})$.

where we have summarised w and b as θ . Given an *activation function* $\zeta : \mathbb{R} \rightarrow \mathbb{R}$, the functions of each layer are given by

$$\begin{aligned}
 f_i^{(1)}(x) &= b_i^{(1)} + \sum_{j=1}^d w_{i,j}^{(1)} x_j, \quad i = 1 \dots N^1 \\
 f_i^{(l)}(x) &= b_i^{(l)} + \sum_{j=1}^{N^{l-1}} w_{i,j}^{(l)} \zeta(f_j^{(l-1)}(x)), \quad i = 1 \dots N^l, \quad l = 2 \dots n \\
 v(x) &= f_1^{(n+1)}(x) = b_1^{(n+1)} + \sum_{j=1}^{N^n} w_{1,j}^{(n+1)} \zeta(f_j^{(n)}(x)).
 \end{aligned} \tag{11}$$

The prior μ_0 is now defined as follows: the individual weights and biases in each layer l are independent and normally distributed, and we emphasise here that the novelty is to choose the variances not uniformly, but to decrease them as one moves into the tail nodes:

$$W_{i,j}^{(1)} \sim \mathcal{N}\left(0, \frac{\sigma_{w^{(1)}}^2}{i^\alpha}\right), \quad W_{i,j}^{(l)} \sim \mathcal{N}\left(0, \frac{\sigma_{w^{(l)}}^2}{(ij)^\alpha}\right) \text{ for } l = 2 \dots n+1, \quad B_i^{(l)} \sim \mathcal{N}\left(0, \frac{\sigma_{b^{(l)}}^2}{i^\alpha}\right), \tag{12}$$

where indices i, j , and l are defined in (10), $\alpha > 1$ is a fixed constant, and $\sigma_{w^{(l)}}^2 > 0$ for each l (to avoid degeneracy of the prior). The reader should note that the prior is invariant with respect to permutation of the input variables, thus avoiding preferential treatment of any of the inputs.

The tuning parameter α controls how much information one believes concentrates on the first nodes. If $\alpha > 1$ we refer to the prior as *trace-class*, coining the term *trace-class neural network priors*. If one believes that many nodes are important, one should choose α close to 1, larger values of α result in strong concentration of information on the first nodes. See Figure 3 for three representative draws from the neural network prior. As the next theorem will show, this allows indeed to define an infinitely wide network by taking $N^l = \infty$, and the variances can be summarised in a diagonal covariance operator \mathcal{C} ; this prior is well-defined on an infinite-dimensional Hilbert space (isometric to ℓ^2), and can thus be used in the algorithms from Section 2. In practice, one truncates the number of nodes within each layer as for the priors described before, or one may randomly switch nodes on and off similarly to the random truncation prior used in Cotter et al. [2013].

We now define the infinite width limit of the network. Given an infinite sequence of weights and biases for the first layer, distributed according to the prior (12), i.e. $\left\{ \left(B_i^{(1)}, W_{i,1}^{(1)}, \dots, W_{i,d}^{(1)} \right) : i \in \mathbb{N} \right\}$, all the functions of the first layer, $\{f_i^{(1)} : i \in \mathbb{N}\}$, are clearly well defined. We define all the functions of the second layer corresponding to an infinite-width first layer to be the following almost sure limits (assuming they exist)

$$F_i^{(2)}(x) = \lim_{N^1 \rightarrow \infty} B_i^{(2)} + \sum_{j=1}^{N^1} W_{i,j}^{(2)} \zeta(f_j^{(1)}(x)) \tag{13}$$

Once we have ascertained the random functions $\{F_i^{(2)} : i \in \mathbb{N}\}$ are well defined, proceeding iteratively, all the functions $\{F_i^{(l)} : i \in \mathbb{N}\}$ of subsequent layers, $l = 3, \dots, n$ and the output layer $F_1^{(n+1)}$ can be defined similarly. The functions in each layer of a finite width network are denoted with lower case to clearly distinguish them from their infinite width versions. For the output layer, the finite network gives $v(x)$ or $f_{n+1}^{(1)}(x)$ while the infinite network gives $V(x)$ or $F_{n+1}^{(1)}(x)$.

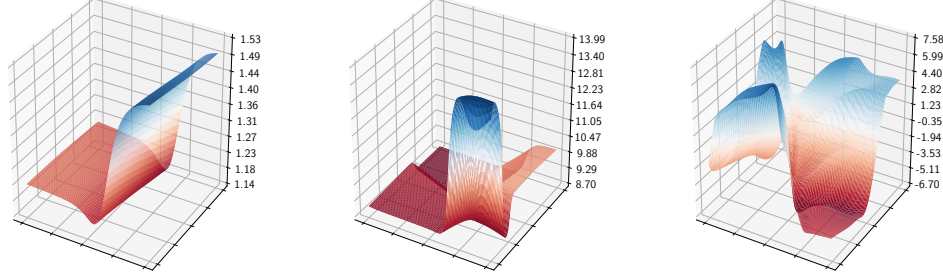


Figure 3: Three samples from the trace-class neural network prior, for a network with 3 fully-connected layers; Tuning parameters are set to $\alpha = 1.5$, $\sigma_w^2 = \sigma_b^2 = 2$ for all $l = 1 \dots n + 1$ (left), $\alpha = 1.5$, $\sigma_w^2 = \sigma_b^2 = 20$ (centre), $\alpha = 1.0001$, $\sigma_w^2 = \sigma_b^2 = 20$ (right). The tuning parameter α controls the complexity of the prior functions, the variances in the layers control the overall variance. Note the difference in the magnitudes on the z -axis.

In what follows, we will often write $v(x) = v_\theta(x)$ to emphasise the dependence of the function samples on the weights and biases. In order to be able to interpret the samples, we generally want the prior to satisfy the following desirable properties:

6. $\forall x \in [0, 1]^d$ one has $|f_i^{(l)}(x)| < \infty$ μ_0 -almost surely, $\mathbb{E}f_i^{(l)}(x) = 0$, and $\exists \sigma_l^2$ such that $\mathbb{E} \left[(f_i^{(l)}(x))^2 \right] < \sigma_l^2 / i^\alpha$, where the expectation is taken with respect to the prior on the parameters of the neural network; in particular this holds for $v(x) = f_1^{(n+1)}(x)$; this assumption ensures that the prior is well-defined;
7. $\forall x, y \in [0, 1]^d \exists c_l \geq 0$ such that $\mathbb{E} \left[(f_i^{(l)}(x) - f_i^{(l)}(y))^2 \right] \leq c_l \|x - y\|^2 / i^\alpha$, with the expectation again taken with respect to the prior; in particular this gives $\mathbb{E} [v(x) - v(y)]^2 \leq c_{n+1} \|x - y\|^2$; this assumption ensures that the functions one samples behave nicely, and that the output function v is sufficiently smooth;
8. $\partial v(x) / \partial x \neq 0$ μ_0 -almost surely, i.e. information from the input layer informs the output layer as a change in the input variables will have an impact on the output variable almost surely.

We now state a theorem which shows that the proposed prior satisfies the desired properties of a prior. To this end, we use an activation function² $\zeta : \mathbb{R} \rightarrow \mathbb{R}$ which satisfies the following condition:

9. ζ is Lipschitz continuous with Lipschitz constant 1 and $\zeta(0) = 0$. In particular this implies $\forall x \in \mathbb{R}$: $|\zeta(x)| < |x|$.³ Furthermore, this implies that ζ is differentiable almost everywhere, with the derivative being essentially bounded by 1.

Theorem 1. *Under Assumption 9, the functions of the layers of the finite-width neural network satisfy Properties 6, 7, and 8. In addition, if the prior is trace-class (i.e. $\alpha > 1$), which implies Property 1, the functions on every layer of the infinite-width neural network (see (13)) exist almost surely and satisfy Properties 6 and 7, when the functions $f_i^{(l)}(x)$ and $v(x)$ therein are replaced with $F_i^{(l)}(x)$ and $V(x)$ defined as in (13).*

The proof can be found in Appendix B.2.

²As will be clear from the proof of theorem 1, one may use different activation functions at different layers, which will then all have to satisfy this assumption.

³The generalisation to arbitrary Lipschitz constants and the implication $\exists c > 0$ such that $\forall x \in \mathbb{R}$: $|\zeta(x)| < c|x|$ is straightforward.

3.1 Identifiability Issues and Remedies

It is well-known that the output function of a standard neural network does not depend on the labeling of functions within each layer. However, unlike a prior that has uniform variances within each layer, swapping nodes $f_i^{(l)}$ and $f_{i+1}^{(l)}$ (effectively by swapping their corresponding weights and biases) will lead from θ to a new θ' such that the prior weights change, and thus avoid the label-switching problem. To facilitate faster mixing by allowing jumps between these different configurations, we propose Algorithm 1, which can be found in Appendix A. The algorithm is well defined in finite widths networks, in which case the acceptance ratio is given by $a(\theta, \vartheta) = \mu_0(\vartheta)/\mu_0(\theta)$, but not in infinite width networks, see Lemma 3 in the Supplementary Material. One remedy is not to swap all the weights of the two selected nodes but only blocks of them, but we did not pursue this approach.

3.2 Illustrative Groundwater Flow Example

Before moving on to more challenging examples, we present an illustrative example, and compare the performance of the neural network prior to the Gaussian prior presented previously. The example is taken from Beskos et al. [2017]⁴. The aim is to recover the permeability of an aquifer. The PDE $-\nabla \cdot (\exp(u(x))\nabla p(x)) = 0$ connects the log-permeability u of a porous medium to the hydraulic head function p with the boundary conditions given by

$$p(x) = x_1 \quad \text{if } x_2 = 0, \quad p(x) = 1 - x_1 \quad \text{if } x_2 = 1, \quad \frac{\partial p(x)}{\partial x_1} = 0 \quad \text{if } x_1 \in \{0, 1\}.$$

To enforce the permeability to be positive, the prior is defined for the log-permeability $u(x)$.

We compare two priors. The first one is a trace-class neural network prior with 100 nodes, Tanh activation function, and a four dimensional input space with the inputs $(x_1, x_2, \sin(x_1), \sin(x_2))$. We set the tuning parameters to $\alpha = 1.001$, $\sigma_{w_1}^2 = \sigma_{b_1}^2 = 100$, $\sigma_{w_2}^2 = 1/30$, and $\sigma_{b_2}^2 = 1/10$. The second prior is a Gaussian measure on $[0, 1]^2$ with the following orthonormal basis and corresponding eigenvalues defined using double indices $i = (i_1, i_2)$:

$$\varphi_i(x) = 2 \cos\left(\pi\left(i_1 + \frac{1}{2}\right)x_1\right) \cos\left(\pi\left(i_2 + \frac{1}{2}\right)x_2\right), \quad \lambda_i^2 = \frac{1}{(\pi^2((i_1 + 1/2)^2 + (i_2 + 1/2)^2))^{1.1}}. \quad (14)$$

In the experiments, we truncated the basis expansion using $1 \leq i_1, i_2 \leq 25$, which gives a similar number of parameters as we used in the neural network example. The true u^* is now defined using the same basis as $u^*(x) = \sum_i u_i^* \varphi_i(x)$ with $u_i^* = \lambda_i \sin((i_1 - 1/2)^2 + (i_2 - 1/2)^2) \cdot \delta[1 \leq i_1, i_2 \leq 10]$. The data is simulated as a noisy observation of the true hydraulic head function p^* as obtained by solving the forward PDE on a 40×40 grid: $y = p^*(x) + \varepsilon$, where $\varepsilon \sim \mathcal{N}(0, 0.01^2)$. We ran pCN using both priors, and solving the forward problem on a 20×20 grid. Both experiments used a similar number of iterations and stored 1000 MCMC samples to obtain the mean estimates in Figure 4. The results in Figure 4 are less accurate than those we will see in the next subsection as far fewer observations are available, which are related to the target function through the PDE, this motivates to validate the results using visual posterior predictive checks as shown in Figure 5.

3.3 Ability to approximate complicated functions

To show that the trace-class neural network prior is able to visually recover relatively complicated functions, we define a function $u^* : [0, 1]^2 \rightarrow \mathbb{R}_+$, and observe this function on a 20×20 grid with independent Gaussian noise $\mathcal{N}(0, 0.01^2)$. The true u^* and the parameters of the prior we used here are the same one as in the example above. As Figure 6 shows, the neural network prior is able to approximate the true u^* when given many, in this example 400, observations.

4 Bayesian Learning of the Optimal Value Function

The solution to a stochastic optimal control problem is known as the *optimal value function* which can be found through Dynamic Programming (DP) (discussed in Section 4.1.) Reinforcement Learning is a popular and practical algorithmic approach for solving stochastic optimal control problems [Sutton and Barto, 2018]. It finds the best control, which is a mapping from states to actions, in an online manner by using noisy estimates of the mathematical expectations to be maximised in DP. Online here refers to the use of the current best learnt control to actuate the system to its next state which is also accompanied by a corresponding stochastic reward. This interaction with the system yields a stochastic process of actions, states and rewards with which DP's mathematical expectations are estimated.

Automating a task can be made easier through the use of expert demonstrations, an approach known as Inverse Reinforcement Learning; see e.g. [Ramachandran and Amir, 2007] for more nuanced details. Given the observed state, actions and rewards from an expert, we can exploit the mathematical formalism of Markov Decision Processes to relate this "data" to the optimal value function of the expert. In a Bayesian approach to this problem, one defines a prior on a function space that includes all admissible value functions. The data observed from the expert's behaviour can then be

⁴While we could not perfectly replicate their results, we aimed to stick as close to their results as possible.

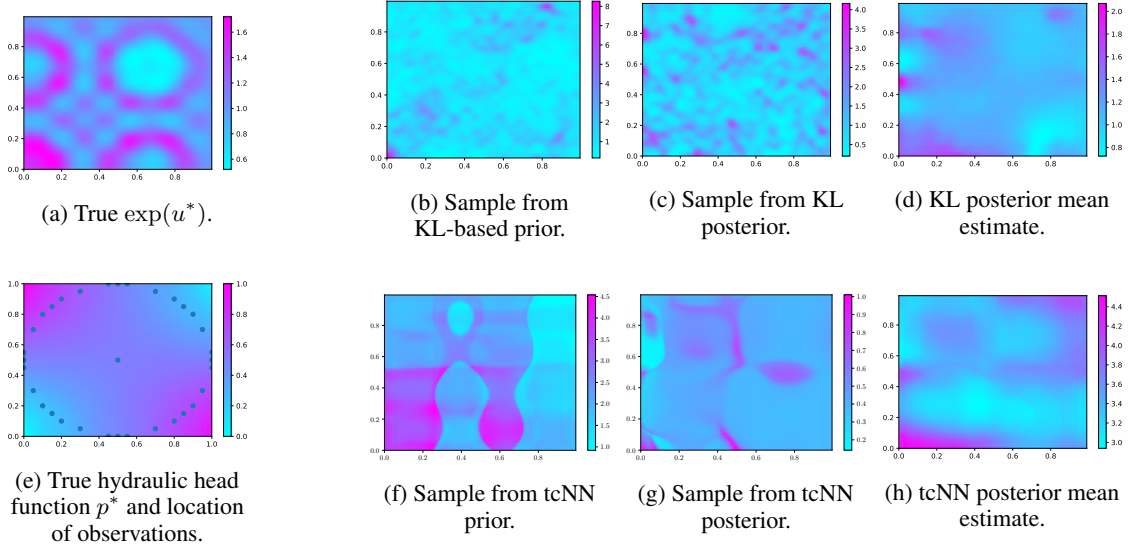


Figure 4: *Left column:* The true log-permeability (a), and its associated hydraulic head function (e) with the location of the 33 observations. *Top row, right columns:* A sample from the Gaussian prior (b), a sample from the associated posterior (c), and the posterior mean estimate obtained using pCN for the Gaussian prior (d). *Bottom row, right columns:* A sample from the trace-class neural network prior (f), a sample from the associated posterior (g), and the posterior mean estimate obtained using pCN for the neural network prior (h).

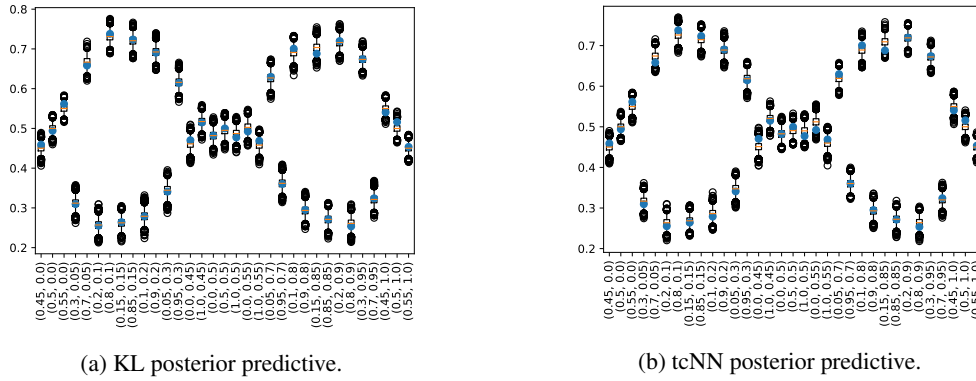


Figure 5: Visual posterior predictive check for both the KL- and tcNN-based posteriors. The observed values at each of the 33 observation locations (see figure 4) are shown as a blue dot, the box plots are 100 samples from the posterior predictive distribution [Gelman et al., 2013, Section 6.3]. Both posteriors show similar predictive performance indicating that they arise from similarly well-suited priors.

used through a suitably defined likelihood [Ramachandran and Amir, 2007] to infer the expert's value function: having the expert's value function at hand allows one to mimic their behaviour and hence defines an approach to automation. For discrete state spaces, Singh et al. [2013] provide a method to quantify the uncertainty of the estimated value function. Here, we will generalise those ideas to continuous state spaces by using priors introduced in the previous section.

4.1 Setup

A *Markov Decision Process* is defined by a controlled Markov chain $\{X_t\}_{t \in \mathbb{N}}$ called the *state process*, the *control process* $\{A_t\}_{t \in \mathbb{N}}$, and an optimality criterion. The state process takes values in a bounded set $\mathcal{X} \subset \mathbb{R}^d$, for simplicity we will consider the domain to be the d -dimensional hypercube $\mathcal{X} = [0, 1]^d$. The control process is \mathcal{A} -valued, where $\mathcal{A} = \{1, \dots, M\}$ is a finite set. Given realisations of the state and actions process until time $T \geq 0$, the state process propagates according to

$$X_{t+1} | (X_{1:t} = x_{1:t}, A_{1:t} = a_{1:t}) \sim p(\cdot | x_t, a_t), \quad (15)$$

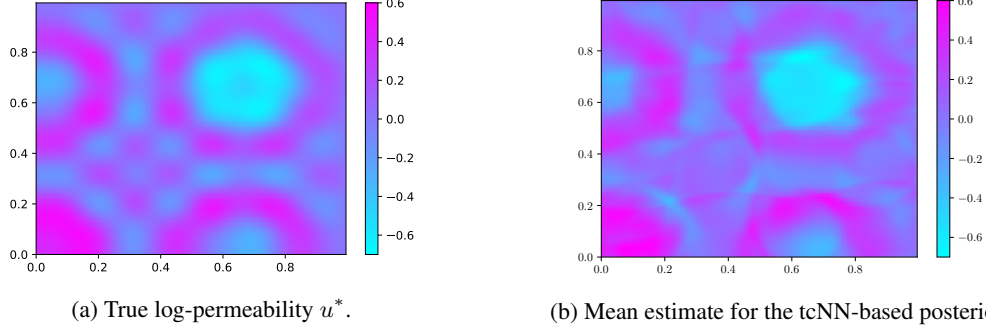


Figure 6: The neural network estimates the true $u^*(x)$ which is noisily observed on every grid point x of a 20×20 grid. In real applications, only few observations will be available, this example simply illustrates that many observations lead to close approximations for the trace-class neural network prior. Note that the functions displayed are shown on a fine grid, a coarse 20×20 sub-grid was used to generate the observations.

where for any state-action pair (x_t, a_t) , $p(\cdot|x_t, a_t)$ is a probability density. In some applications, the state dynamics are deterministic, and thus there exists a map \mathcal{T} such that $X_{t+1} = \mathcal{T}(x_t, a_t)$. The action process depends on a *policy* $\mu : \mathcal{X} \rightarrow \mathcal{A}$ which is a deterministic mapping from the state space into the action space: $A_t|(X_{1:t} = x_{1:t}, A_{1:t-1} = a_{1:t-1}) \sim \delta_{\mu(x_t)}(\cdot)$. As there are many possible mappings $\mu : \mathcal{X} \mapsto \mathcal{A}$, we assume the agent executes a policy that is in some way optimal. To be more precise, let $r : \mathcal{X} \rightarrow \mathbb{R}$ be the *reward function*, then the *accumulated reward* given a policy and an initial state $X_1 = x_1$ is

$$C_\mu(x_1) = \mathbb{E}_\mu \left[\sum_{t=1}^{\infty} \beta^t r(X_t) | X_1 = x_1 \right],$$

where $\beta \in (0, 1)$ is a discount factor. The discount factor serves two purposes: it ensures that the expectation is well defined, and also lets early actions be more important than later actions, see Kaelbling et al. [1996] for a more detailed discussion. A policy μ^* is *optimal* if $C_{\mu^*}(x_1) \geq C_\mu(x_1)$ for all (μ, x_1) and the optimal policy can be found through the solution of Bellman's fixed-point equation [Bellman, 1952]. The function $v : \mathcal{X} \rightarrow \mathbb{R}$, which is the fixed-point solution to

$$v(x) = \max_{a \in \mathcal{A}} \left[r(x) + \beta \int_{\mathcal{X}} p(x'|x, a) v(x') dx' \right],$$

is called the *optimal value function* [Bertsekas, 1995] and corresponding optimal policy by

$$\mu^*(x) = \arg \max_{a \in \mathcal{A}} \left[\int_{\mathcal{X}} p(x'|x, a) v(x') dx' \right], \quad (16)$$

that is, the optimal action at any state is the one that maximises the expected value function at the next state.

4.2 Likelihood definition

The above decision making process gives optimal actions, but a human expert may occasionally pick non-optimal ones. To model imperfect action selections, noise is added to (16). At each time step the chosen action is a random variable given by

$$A_t(x_t) = \arg \max_{a \in \mathcal{A}} \left[\int_{\mathcal{X}} p(x'|x_t, a) v(x') dx' + \epsilon_t(a) \right], \quad (17)$$

where we assume $\epsilon_t \sim \mathcal{N}(0, \sigma^2 I_{M \times M})$. The Gaussian choice simplifies numerical calculations, and it is reasonable to assume that the variances for different actions are independent and identically distributed, but this assumption can be relaxed. When the state dynamics are deterministic, action selections occur according to

$$A_t(x_t) = \arg \max_{a \in \mathcal{A}} [v(\mathcal{T}(x_t, a)) + \epsilon_t(a)], \quad (18)$$

Our goal from now on will be to recover the optimal value function, and quantify the uncertainty thereof, by using the Hilbert space MCMC methods and the priors discussed in Sections 2 and 3.

The data consists of a collection of state-action pairs $y = \{y_t\}_{t=1}^T = \{(x_t, a_t)\}_{t=1}^T$ and the aim is to infer the value function (and thus the policy through (16)) that leads to the actions a_t for the current state x_t . Using the noisy action selection procedure (17), the likelihood is

$$\mathcal{L}(y|v, \sigma) = \prod_{t=1}^T p(a_t|x_t, v, \sigma) = \prod_{t=1}^T p(a_t|v_t, \sigma), \quad (19)$$

by defining the vector v_t , containing the relevant evaluations of the value function to calculate the likelihood at y_t , i.e. using equation (18), the k -th entry of v_t is the evaluation of the value function $v(\cdot)$ at the location $T(x_t, k)$, corresponding to starting at x_t and taking action $a = k \in \mathcal{A}$.

For a single observation $y_t = (x_t, a_t)$, we now drop the subscript t to simplify notation, and assume wlog that the optimal action is action $k = 1$, permuting the labels if necessary. The probability $p(a = 1|v, \sigma)$ (where v is now a vector and $p(a|v, \sigma)$ is a probability mass function) can be computed using (17) by

$$p(a = 1|v, \sigma) = \int \mathbb{1}_{\{u \in \mathbb{R}^d: u_1 \geq u_j \forall j \neq 1\}} \mathcal{N}(u; v, \sigma^2 I_{M \times M}) du. \quad (20)$$

To compute this term, we make use of the fact that the value of the integral is the same as the probability $\mathbb{P}(X_1 > X_j, \forall j \neq 1)$, where $X_k \sim \mathcal{N}(v(T(x, k)), \sigma^2)$. This can be computed numerically using the pdf $\phi_1(\cdot)$ of X_1 and cdfs $\Phi_j(\cdot)$ of the respective X_j :

$$p(a = 1|v, \sigma) = \int_{-\infty}^{\infty} \phi_1(t) \Phi_2(t) \dots \Phi_M(t) dt \quad (21)$$

$$= \frac{1}{\sigma} \int_{-\infty}^{\infty} \phi\left(\frac{t-v_1}{\sigma}\right) \prod_{j=2}^M \Phi\left(\frac{t-v_j}{\sigma}\right) dt. \quad (22)$$

If the noise in (17) is not diagonal, this simplification cannot be made, and the integral (20) is harder to compute. More advanced numerical methods exist to efficiently calculate such integrals using Monte-Carlo simulations [Genz, 1992].

4.3 Likelihood gradient

Following from (22) we can compute the gradient of the likelihood in a data point (x_t, a_t) with respect to v_t . We again assume wlog that $a_t = 1 \in \mathcal{A}$ (by swapping the label of the first and the best action if necessary), and drop the subscript t , emphasising that v_k is the k -th entry of the vector v . The partial derivatives with respect to the v_k are given by

$$\frac{\partial}{\partial v_1} p(a = 1|v, \sigma) = \frac{1}{\sigma} \int_{-\infty}^{\infty} \frac{t-v_1}{\sigma^2} \phi\left(\frac{t-v_1}{\sigma}\right) \prod_{j=2}^M \Phi\left(\frac{t-v_j}{\sigma}\right) dt \quad (23)$$

$$\frac{\partial}{\partial v_k} p(a = 1|v, \sigma) = -\frac{1}{\sigma^2} \int_{-\infty}^{\infty} \phi\left(\frac{t-v_1}{\sigma}\right) \phi\left(\frac{t-v_k}{\sigma}\right) \prod_{j=2, j \neq k}^M \Phi\left(\frac{t-v_j}{\sigma}\right) dt \quad k = 2 \dots M \quad (24)$$

$$= -\frac{1}{\sigma^2} \phi\left(\frac{v_1-v_k}{\sqrt{2}\sigma}\right) \int_{-\infty}^{\infty} \phi\left(\frac{t-\frac{v_k+v_1}{2}}{\frac{\sigma}{\sqrt{2}}}\right) \prod_{j=2, j \neq k}^M \Phi\left(\frac{t-v_j}{\sigma}\right) dt, \quad (25)$$

where the last identity follows from the product of two Gaussian pdfs. This allows us, when using the neural network prior, to compute the gradient of the log-likelihood with respect to the parameters of the neural network, θ , using backpropagation. We emphasise that the vector $v = v(\theta)$ depends on these parameters, justifying the calculation of the Jacobian $\mathcal{D}_\theta v$. Using the chain rule, we get

$$\nabla_\theta \log p(a = 1|v, \sigma) = \frac{\nabla_v p(a = 1|v, \sigma)}{p(a = 1|v, \sigma)} = \frac{(\mathcal{D}_\theta v)^T \nabla_v p(a = 1|v, \sigma)}{p(a = 1|v, \sigma)}. \quad (26)$$

To get the entire gradient of the log-likelihood, we simply need to sum over all data points:

$$\nabla_\theta \ell(y|v, \sigma) = \nabla_\theta \log \left(\prod_{t=1}^T p(a_t|v_t, \sigma) \right) = \nabla_\theta \sum_{t=1}^T \log p(a_t|v_t, \sigma) = \sum_{t=1}^T \nabla_\theta \log p(a_t|v_t, \sigma), \quad (27)$$

where we only need to keep in mind the permutation in the actions when using (26).

When calculating (26), we note that $1 \cdot \nabla_v p(a|v, \sigma) = 0$ by translation invariance of v : $\mathcal{L}(y|v, \sigma) = \mathcal{L}(y|v + c, \sigma)$ for any constant function c , i.e. $c(x) = c(x')$ for all $x, x' \in \mathcal{X}$. To avoid numerical instabilities when calculating

the gradient, due to large absolute values, we can ensure that the mean of these gradients is 0 by using the following modification, which we observed to enhance the performance in practice:

$$(26) = \frac{\sum_{k=1}^M ((\mathcal{D}_\theta v)^T)_k (\frac{\partial}{\partial v_k} p(a=1|v, \sigma) - \sum_{k=1}^M \frac{\partial}{\partial v_k} p(a=1|v, \sigma))}{p(a=1|v, \sigma)}. \quad (28)$$

The following theorem justifies the use of this likelihood in the function space MCMC setting:

Theorem 2. *The log-likelihood $\ell(y|v, \sigma) = \log \mathcal{L}(y|v, \sigma)$ defined in (19) satisfies Assumptions 3 and 4, where $v \in \mathcal{H} = L^2$.*

The proof can be found in Appendix B.4. We also note that when using the trace-class neural network prior from Section 3, the statements remain true if the likelihood is seen as a function of the parameters θ of the neural network:

Lemma 1. *The log-likelihood $\ell(y|v_\theta, \sigma)$ defined in (19) satisfies Assumptions 3 and 4, where now inference is over the weights and biases, $\theta \in \mathcal{H} = \ell^2$.*

Proof. As v is a Lipschitz continuous function of θ , $\ell(y|v(\theta), \sigma)$, as a composition of Lipschitz continuous functions, is also Lipschitz continuous in θ ; and, with an activation function satisfying Condition 9, v grows at most polynomial in θ . \square

The next theorem ensures that the pCNL algorithm is well-defined for both priors by making sure that proposals are μ_0 -almost surely in the image of the prior:

Theorem 3. *Let $\mathcal{N}(0, \mathcal{C})$ be a Gaussian prior for either the parameterisation in Theorem 2 or that in Lemma 1. For any $u \sim \mathcal{N}(0, \mathcal{C})$, we have $\mathcal{N}(\mathcal{CD}\ell(u), \mathcal{C}) \simeq \mathcal{N}(0, \mathcal{C})$, almost surely with respect to the data, i.e. the two Gaussian measures are absolutely continuous with respect to one another. In other words, Condition 5 holds, i.e. the preconditioned gradient of the log-likelihood is in the Cameron-Martin space of the prior.*

As the theorem holds for either parameterisation, for the KL-prior $D\ell(u)$ should be understood as the collection of derivatives with respect to the ξ_i and the prior is over $\mathcal{H} = L^2$, whereas for the trace-class neural network prior, $D\ell(u)$ is the collection of derivatives with respect to each weight and bias and the inference is over the parameters of the neural network which are elements of $\mathcal{H} = \ell^2$. The proof can be found in Appendix B.5.

5 Numerical Illustrations

This section aims to validate the theory, and highlight the applicability of the proposed priors and methodology. In particular, Section 5.2 confirms that, empirically, as the layer width for the trace-class neural network prior grows, the acceptance probability does not go to 0, a property known as ‘stable under mesh-refinement’ or ‘dimension-independence’. Section 5.3 compares the proposed trace-class neural network (tcNN) prior to a standard BNN and a KL prior, it highlights that, unlike the KL prior, the tcNN is scalable to higher-dimensional domains; and Section 5.4 shows that the posteriors can learn and mimic policies, thus justifying the use of these priors in the reinforcement learning setup. The code is available at <https://github.com/TorbenSell/trace-class-neural-networks>.

Throughout we use the Fourier basis (5) as the series expansion of choice when using the KL based prior, as this proved to be a good choice for reinforcement learning problems [Konidaris et al., 2011]. As a tuning parameter for the corresponding eigenvalues we set $\alpha = 2$ in (6), forcing the samples to be very smooth which we expect to be a sensible choice in the discussed control problems. For the tcNN prior we used fully connected layers with tanh activation functions, and set $\sigma_{b^{(l)}}^2 = \sigma_{w^{(l)}}^2 = 2$ and $\alpha = 1.5$, this again results in smooth sample functions. For the standard BNN we used the same architecture and set $\alpha = 0$ to get a constant variance sequence and $\sigma_{b^{(l)}}^2 = \sigma_{w^{(l)}}^2 = 1/3$.

5.1 Control Problems: Setup

We set the scene by briefly describing the setup of the control problems which we use in the experiments, a detailed description can be found in the Supplementary Material.

The first example is the popular mountaincar problem. A car is to drive up a mountainslope to reach a flag, but needs to gain momentum first by driving up the opposite mountain slope. See the left panel of Figure 7 for an illustration. The state space is the two-dimensional domain $\mathcal{X} = [-1.2, 0.6] \times [-0.07, 0.07]$ describing the vehicle’s position and velocity, and the action space contains three possible actions: $\mathcal{A} = \{-1, 0, 1\}$, representing exerting force to the left, no force, and exerting force to the right, respectively. The likelihood (22) arises from $T = 50$ observations of state-action pairs, the data generating process is described in the Supplementary Material. The noise level in the likelihood is set to $\sigma = 0.1$.

The second example is the HalfCheetah example from the MuJoCo library [Todorov et al., 2012], where an agent controls a two-dimensional cheetah with the aim to ‘run’ as fast as possible. For this example, the state space \mathcal{X} is 17-dimensional and the action space contains 8 possible actions. The likelihood (22) arises from $T = 100$ observations, we again refer to the Supplementary Material for the data generating process, and set the noise level in the likelihood to $\sigma = 0.1$. The right panel of Figure 7 shows the HalfCheetah.

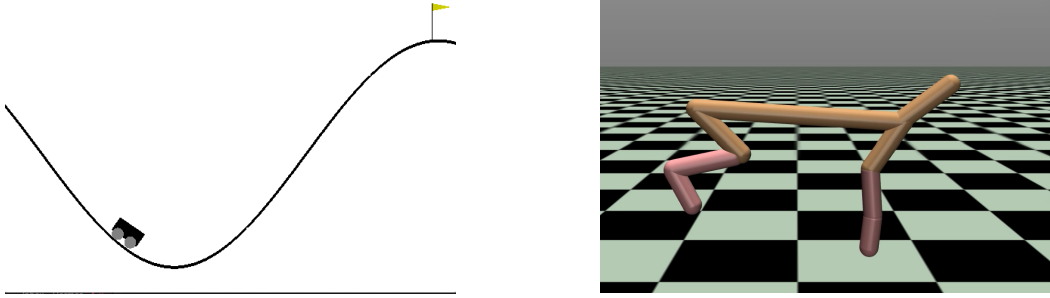


Figure 7: *Left*: The setup for the mountaincar example. The car’s goal is to reach the flag in as few steps as possible. The slope on the right is too steep to simply drive up the mountain, the car therefore has to gain momentum by going up the hill on the left first. *Right*: The HalfCheetah has states x_t in \mathbb{R}^{17} . Its goal is to run to the right as quickly as possible, while not moving its body parts more than necessary.

5.2 Dimension independence of trace-class neural network prior under mesh-refinement

We ran pCN for different network widths on the mountaincar example. The network used has $l = 3$ hidden layers. As stated before, the tuning parameters in the prior are set to $\sigma_{b^{(l)}}^2 = \sigma_{w^{(l)}}^2 = 2$, and $\alpha = 1.5$. Table 1 displays the acceptance probability of pCN for a fixed step size when targeting the posteriors arising from the mountaincar likelihood and firstly the trace-class neural network prior and secondly a standard Bayesian neural network. The latter is characterised by setting $\alpha = 0$ in (12), resulting in a constant sequence of variances per layer. The other tuning parameters for the standard Bayesian neural network were set to $\sigma_{b^{(l)}}^2 = \sigma_{w^{(l)}}^2 = 1/3$. The step sizes chosen were $\beta = 1/10$ for the tcNN, $\beta = 1/7$ for the standard BNN.

$N^{(l)}$, for all l	10	20	30	40	50	60	70	80	90	100
Acc. ratio (tcNN)	22.8	24.0	23.5	22.1	22.2	23.1	23.9	23.4	23.0	23.9
Acc. ratio (BNN)	26.8	15.6	9.1	5.1	2.7	1.5	0.86	0.50	0.36	0.18
Total # of param.	261	921	1981	3441	5301	7561	10221	13281	16741	20601

Table 1: Acceptance ratios in % for both the trace-class neural network (tcNN) and standard Bayesian neural network (BNN) and total number of parameters (weights and biases) for different layer widths. 3 fully connected layers were used, and pCN was run over 3 hours for each of the layer widths. Notably the acceptance probability for the trace-class neural network proposed in this paper does not degenerate as more nodes are included per layer.

5.3 Comparison of priors

To compare the trace-class neural network prior to the Karhunen-Loève prior, we used a large number of parameters for each, such that the error from truncating after finitely many nodes, or finitely many terms, is negligible. For both the mountaincar and the HalfCheetah example, we used the same trace-class neural network prior, with 3 hidden layers, and 100 nodes per layer, resulting in 20,601 parameters to be estimated for the mountaincar example, and 22,101 for the HalfCheetah example. For the Karhunen-Loève prior in the mountaincar example we set the truncation parameter to $k_{max} = 70$ for (5) with eigenvalues (6) (recall that here $\alpha = 2$), resulting in a total of 19,880 coefficients to be estimated. For the KL prior in the HalfCheetah example we used approximation (3), and otherwise the same eigenfunctions and eigenvalues; due to the higher domain dimension $d = 17$, one would have to estimate 2,667,980 parameters. As this is too memory-expensive for the computer used for the experiments, we used $k_{max} = 10$ in the HalfCheetah example, resulting in 54,740 parameters to be estimated. Note that this increase in parameters to be estimated is already due to the approximation (3) being used, and additionally truncating the expansions after fewer terms, highlighting the benefits of the dimension-robustness of the trace-class neural network prior.

To assess the quality of the priors, we ran pCN using 50 (for the mountaincar) and 100 (for the HalfCheetah) data points. For the mountaincar example, we fixed five test points z_j , $j = 1, \dots, 5$ independent of the training data, and compared the posteriors by evaluating $v(z_j)$ at these new locations as estimated through MCMC runs. The top row in Figure 8 shows the resulting uncertainty estimates. As the value function is invariant under translations, we adjusted all samples such that they take the value 0 at the state which the optimal action a_{opt} takes one to:

$$v_{1:M}^{\text{centered}} = v_{1:M} - v_{a_{opt}} \cdot \mathbf{1}, \quad (29)$$

where $\mathbf{1}$ denotes a vector of ones. For the HalfCheetah example, we looked at one test point for illustration, see the bottom row in Figure 8, and summarised the performance on another 100 test points (independent of the training data)

Decision by	KL samples	BNN samples	tcNN samples	KL mean	BNN mean	tcNN mean
Optimal	20.1%	18.1%	32.1%	25%	20%	42%
Non-optimal	79.9%	81.9%	67.9%	75%	80%	58%

Table 2: Actions picked using Equation 17 with v a posterior sample or the estimated posterior mean. The trace-class neural network prior outperforms the approximate KL and the standard BNN prior. The optimal action is computed using the same policy used to simulate data, see Section 5.1, the test points chosen at random from a representative episode of a HalfCheetah run. A random prediction would result in a success rate of 12.5%.

in the Table 2, where we compared how the respective samples from the posterior do, as well as how the mean of all samples from the posterior in Section 5.4 (with a smaller number of nodes for the tcNN prior, and fewer active terms in the KL prior⁵) does on predicting the correct action (last two columns). Not surprisingly, the mean function is better at picking the correct action.

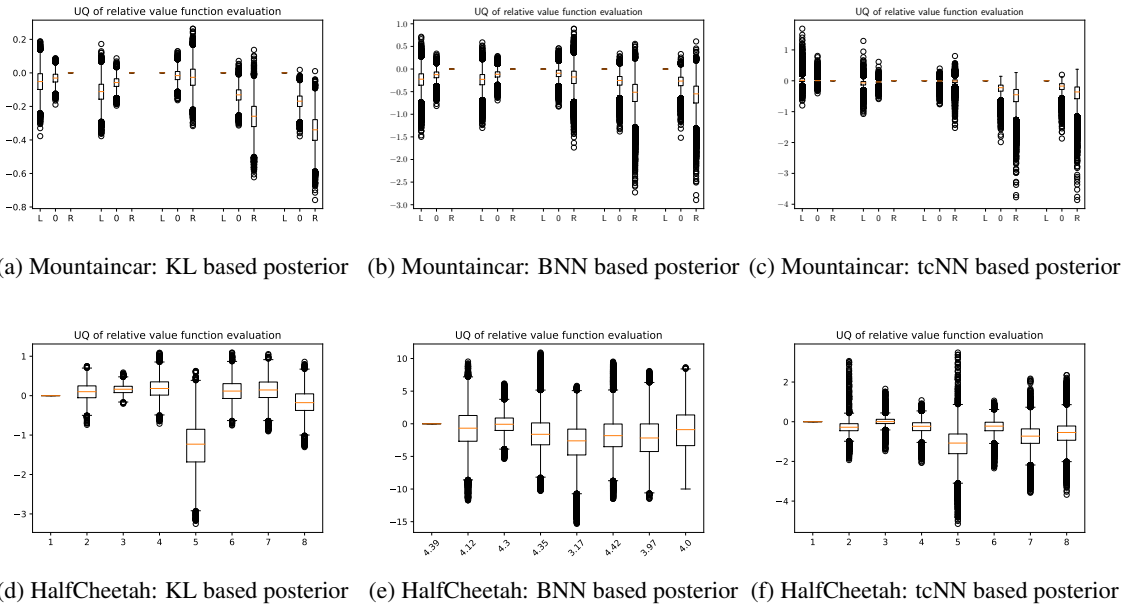


Figure 8: Uncertainty estimates arising from the two different priors for the mountaincar and the HalfCheetah examples. *Top row*: Mountaincar example. In each plot, five different states are looked at, the estimates of the value functions are shown, standardised such that the optimal action has value 0 always using (29). None of the posteriors can make a clear judgement as to what the optimal actions for the first three shown states are, as the boxplots illustrate the uncertainty when predicting the best action. For the fourth and fifth states, all posteriors suggest a clear decision for action ‘Left’. The reader should note that the KL, the BNN, and the tcNN posteriors behave similarly in that they are uncertain in the first three states, and very decisive in the last two states.

Bottom row: HalfCheetah example. The optimal action is the first one in both plots, and samples are again normalised using (29) such that they take the value 0 at the state the optimal value takes one to. The BNN and tcNN posteriors correctly estimates the optimal action, the KL posterior doesn’t.

5.4 Ability to Learn Policy

To asses if the posteriors can truly learn an agent’s behaviour, we used the priors with a smaller number of parameters, and stored 1000 samples for each posterior. We then used these samples to obtain a mean value function which was used for decision making. For the trace-class neural network prior we used 3 layers with 10 nodes per layer for both examples (resulting in 261 parameters for the mountaincar example and 411 for the HalfCheetah); for the KL prior we used $k_{max} = 7$ for the mountaincar example (giving a total of 224 parameters), and $k_{max} = 5$ in the HalfCheetah example (a total of 8, 730 parameters). While the number of parameters can theoretically be chosen infinitely large, we

⁵To calculate the mean function it is necessary to store the samples which (due to ther used computer’s limited memory capacity) would not be feasible for the very wide layer prior, nor all the terms in the KL prior.

truncated the layers and expansions earlier as we only had a very limited computational budget available. In general, where to truncate is an interesting model choice problem, and we found that for our problems the parameters described above yield very good approximations to a model with many more parameters. We thus chose to run the simplified model rather than a model with many more parameters, allowing many more stored MCMC posterior samples (1000 in this case) in the same wall-clock time. The results are summarised in Figure 9.

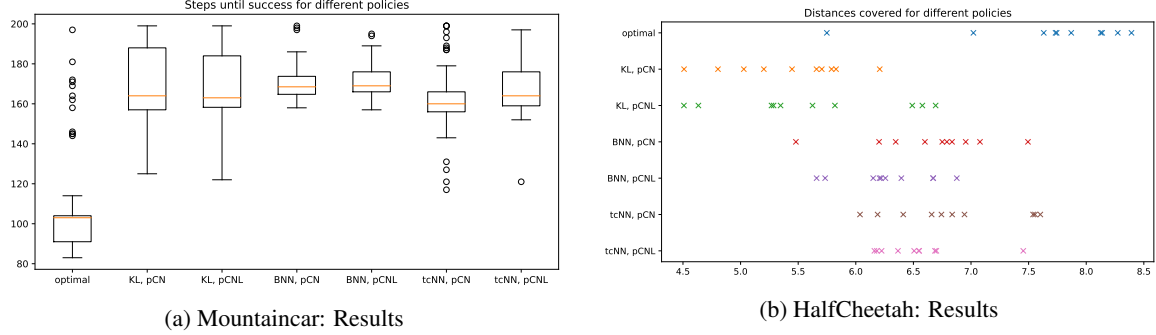


Figure 9: Results for the policy learning experiment.

Left: Mountaincar example. The number of steps until success is shown for different posteriors. If the goal was not reached after 200 steps, the run was counted as failure. Out of 100 runs, the policy following the KL posterior when using pCN gave 34 failures (24 when using pCNL), the standard BNN posterior gave 81 (pCN) and 80 (pCNL) failures, and the tcNN posteriors gave 23 (for the posterior estimates obtained using pCN) and 25 (pCNL).

Right: HalfCheetah example. The different policies arising from the KL posterior (obtained once using pCN, once using pCNL), a standard BNN posterior, and the tcNN posterior were controlling the agent over 10 runs with 100 time steps. The distances covered per run are shown in the plot.

6 Conclusion and Outlook

This paper addresses the problem of effective Bayesian inference for unknown functions with higher dimensional domains. Unlike priors which require an orthogonal basis for the function space and scale exponentially in the domain dimension, our proposed trace-class neural network prior easily scales to higher-dimensional domains as the dependence on the domain dimension is linear. When using the pCN sampling method, this prior also satisfies the desired property of being stable under mesh-refinement, in the sense that the acceptance probability of pCN does not degenerate to 0 when using more parameters for the neural network. Various questions remain unanswered though, and interesting directions of research open up: are there suitable further generalisations of the proposed prior, e.g. heavy-tailed or hierarchical ones, which still satisfy the desired properties, enabling the use of these priors in the function space setting? What are the optimal settings for the tuning parameters $\sigma_{w^{(l)}}^2$, $\sigma_{b^{(l)}}^2$ and α ?

Can one obtain contraction rates to ensure the concentration of the posterior samples around the true functions? A first idea here is to exploit the various generalisations of the universal approximation theorem [Scarselli and Tsoi, 1998], and combine them with the proof methodology used in this paper.

We further introduced a likelihood suitable for Bayesian reinforcement learning where the underlying Markov decision process has a continuous state-space, and thus the unknown value function to be estimated has domain \mathbb{R}^d as opposed to a discrete set. An interesting research direction is to generalise this to continuous action spaces as well.

Finally, we underscored the theory with numerical illustrations, illustrating the applicability of the prior in various control problems.

References

- Sergios Agapiou, Stig Larsson, and Andrew M Stuart. Posterior contraction rates for the bayesian approach to linear ill-posed inverse problems. *Stochastic Processes and Their Applications*, 123(10):3828–3860, 2013.
- Krishna B Athreya and Peter Ney. A new approach to the limit theory of recurrent markov chains. *Transactions of the American Mathematical Society*, 245:493–501, 1978.
- Richard Bellman. On the theory of dynamic programming. *Proceedings of the National Academy of Sciences of the United States of America*, 38(8):716, 1952.
- Dimitri P Bertsekas. *Dynamic Programming and Optimal Control*, volume 1. Athena scientific Belmont, MA, 1995.

- Alexandros Beskos, Gareth Roberts, Andrew Stuart, and Jochen Voss. Mcmc methods for diffusion bridges. *Stochastics and Dynamics*, 8(03):319–350, 2008.
- Alexandros Beskos, Mark Girolami, Shiwei Lan, Patrick E Farrell, and Andrew M Stuart. Geometric mcmc for infinite-dimensional inverse problems. *Journal of Computational Physics*, 335:327–351, 2017.
- Greg Brockman, Vicki Cheung, Ludwig Pettersson, Jonas Schneider, John Schulman, Jie Tang, and Wojciech Zaremba. Openai gym, 2016.
- Steve Brooks, Andrew Gelman, Galin Jones, and Xiao-Li Meng. *Handbook of Markov Chain Monte Carlo*. CRC press, 2011.
- Robert H Cameron and William T Martin. Transformations of wiener integrals under translations. *Annals of Mathematics*, pages 386–396, 1944.
- Simon L Cotter, Gareth O Roberts, Andrew M Stuart, and David White. Mcmc methods for functions: Modifying old algorithms to make them faster. *Statistical Science*, pages 424–446, 2013.
- Tiangang Cui, Kody JH Law, and Youssef M Marzouk. Dimension-independent likelihood-informed mcmc. *Journal of Computational Physics*, 304:109–137, 2016.
- Giuseppe Da Prato and Jerzy Zabczyk. *Stochastic Equations in Infinite Dimensions*. Cambridge university press, 2014.
- Andreas Damianou and Neil Lawrence. Deep gaussian processes. In *Artificial Intelligence and Statistics*, pages 207–215, 2013.
- Masoumeh Dashti, Stephen Harris, and Andrew Stuart. Besov priors for bayesian inverse problems. *arXiv preprint arXiv:1105.0889*, 2011.
- Masoumeh Dashti, Kody JH Law, Andrew M Stuart, and Jochen Voss. Map estimators and their consistency in bayesian nonparametric inverse problems. *Inverse Problems*, 29(9):095017, 2013.
- Matthew M Dunlop, Mark A Girolami, Andrew M Stuart, and Aretha L Teckentrup. How deep are deep gaussian processes? *The Journal of Machine Learning Research*, 19(1):2100–2145, 2018.
- Andreas Eberle et al. Error bounds for metropolis–hastings algorithms applied to perturbations of gaussian measures in high dimensions. *The Annals of Applied Probability*, 24(1):337–377, 2014.
- Andrew Gelman, John B Carlin, Hal S Stern, David B Dunson, Aki Vehtari, and Donald B Rubin. *Bayesian Data Analysis*. CRC press, 2013.
- Alan Genz. Numerical computation of multivariate normal probabilities. *Journal of computational and graphical statistics*, 1(2):141–149, 1992.
- Evarist Giné and Richard Nickl. *Mathematical Foundations of Infinite-dimensional Statistical Models*, volume 40. Cambridge University Press, 2016.
- Martin Hairer, Andrew M Stuart, Sebastian J Vollmer, et al. Spectral gaps for a metropolis–hastings algorithm in infinite dimensions. *The Annals of Applied Probability*, 24(6):2455–2490, 2014.
- Enkelejd Hashorva. Asymptotics and bounds for multivariate gaussian tails. *Journal of theoretical probability*, 18(1):79–97, 2005.
- W Keith Hastings. Monte carlo sampling methods using markov chains and their applications. 1970.
- Kurt Hornik. Approximation capabilities of multilayer feedforward networks. *Neural networks*, 4(2):251–257, 1991.
- Bamdad Hosseini. Well-posed bayesian inverse problems with infinitely divisible and heavy-tailed prior measures. *SIAM/ASA Journal on Uncertainty Quantification*, 5(1):1024–1060, 2017.
- Bamdad Hosseini and Nilima Nigam. Well-posed bayesian inverse problems: Priors with exponential tails. *SIAM/ASA Journal on Uncertainty Quantification*, 5(1):436–465, 2017.
- Marco A Iglesias, Kody JH Law, and Andrew M Stuart. Evaluation of gaussian approximations for data assimilation in reservoir models. *Computational Geosciences*, 17(5):851–885, 2013.
- Arieh Iserles and Syvert P Nørsett. From high oscillation to rapid approximation iii: Multivariate expansions. *IMA journal of numerical analysis*, 29(4):882–916, 2009.
- Leslie Pack Kaelbling, Michael L Littman, and Andrew W Moore. Reinforcement learning: A survey. *Journal of artificial intelligence research*, 4:237–285, 1996.
- Bartek T Knapik, Aad W Van Der Vaart, J Harry van Zanten, et al. Bayesian inverse problems with gaussian priors. *The Annals of Statistics*, 39(5):2626–2657, 2011.

- George Konidaris, Sarah Osentoski, and Philip Thomas. Value function approximation in reinforcement learning using the fourier basis. In *Twenty-fifth AAAI conference on artificial intelligence*, 2011.
- Benedict Leimkuhler, Charles Matthews, and Tiffany Vlaar. Partitioned integrators for thermodynamic parameterization of neural networks. *arXiv preprint arXiv:1908.11843*, 2019.
- Zachary C Lipton. The mythos of model interpretability. *Queue*, 16(3):31–57, 2018.
- Alexander G de G Matthews, Mark Rowland, Jiri Hron, Richard E Turner, and Zoubin Ghahramani. Gaussian process behaviour in wide deep neural networks. *arXiv preprint arXiv:1804.11271*, 2018.
- Brent Minchew, Mark Simons, Scott Hensley, Helgi Björnsson, and Finnur Pálsson. Early melt season velocity fields of langjökull and hofsjökull, central iceland. *Journal of Glaciology*, 61(226):253–266, 2015.
- Radford M Neal. *Bayesian Learning for Neural Networks*, volume 118. Springer Science & Business Media, 2012.
- RM Neal. Bayesian learning for neural networks [phd thesis]. *Toronto, Ontario, Canada: Department of Computer Science, University of Toronto*, 1995.
- RM Neal. Regression and classification using gaussian process priors. *Bayesian statistics*, 6:475, 1998.
- Richard Nickl and Matteo Giordano. Consistency of bayesian inference with gaussian process priors in an elliptic inverse problem. *Inverse Problems*, 2020.
- ALFIO Quarteroni, Andrea Manzoni, and Christian Vergara. The cardiovascular system: Mathematical modelling, numerical algorithms and clinical applications. *Acta Numerica*, 26:365–590, 2017.
- Deepak Ramachandran and Eyal Amir. Bayesian inverse reinforcement learning. In *IJCAI*, volume 7, pages 2586–2591, 2007.
- Gareth O Roberts and Jeffrey S Rosenthal. Optimal scaling of discrete approximations to langevin diffusions. *Journal of the Royal Statistical Society: Series B (Statistical Methodology)*, 60(1):255–268, 1998.
- Gareth O Roberts, Richard L Tweedie, et al. Exponential convergence of langevin distributions and their discrete approximations. *Bernoulli*, 2(4):341–363, 1996.
- Gareth O Roberts, Jeffrey S Rosenthal, et al. Optimal scaling for various metropolis–hastings algorithms. *Statistical science*, 16(4):351–367, 2001.
- I Richard Savage. Mills’ ratio for multivariate normal distributions. *J. Res. Nat. Bur. Standards Sect. B*, 66:93–96, 1962.
- Franco Scarselli and Ah Chung Tsoi. Universal approximation using feedforward neural networks: A survey of some existing methods, and some new results. *Neural networks*, 11(1):15–37, 1998.
- Sumeetpal S Singh, Nicolas Chopin, and Nick Whiteley. Bayesian learning of noisy markov decision processes. *ACM Transactions on Modeling and Computer Simulation (TOMACS)*, 23(1):4, 2013.
- Ilya M Sobol. Sensitivity estimates for nonlinear mathematical models. *Mathematical modelling and computational experiments*, 1(4):407–414, 1993.
- Andrew M Stuart. Inverse problems: A bayesian perspective. *Acta numerica*, 19:451–559, 2010.
- Richard S Sutton and Andrew G Barto. *Reinforcement Learning: An Introduction*. MIT press, 2018.
- Luke Tierney et al. A note on metropolis–hastings kernels for general state spaces. *The Annals of Applied Probability*, 8(1):1–9, 1998.
- Emanuel Todorov, Tom Erez, and Yuval Tassa. Mujoco: A physics engine for model-based control. In *2012 IEEE/RSJ International Conference on Intelligent Robots and Systems*, pages 5026–5033. IEEE, 2012.
- Aad W van der Vaart, J Harry van Zanten, et al. Rates of contraction of posterior distributions based on gaussian process priors. *The Annals of Statistics*, 36(3):1435–1463, 2008.
- Max Welling and Yee W Teh. Bayesian learning via stochastic gradient langevin dynamics. In *Proceedings of the 28th international conference on machine learning (ICML-11)*, pages 681–688, 2011.
- Florian Wenzel, Kevin Roth, Bastiaan S Veeling, Jakub Świątkowski, Linh Tran, Stephan Mandt, Jasper Snoek, Tim Salimans, Rodolphe Jenatton, and Sebastian Nowozin. How good is the bayes posterior in deep neural networks really? *arXiv preprint arXiv:2002.02405*, 2020.
- Przemyslaw Wojtaszczyk. *A Mathematical Introduction to Wavelets*, volume 37. Cambridge University Press, 1997.
- Zhiqing Xiao. *Reinforcement Learning: Theory and Python Implementation*. China Machine Press, 2019.

A NodeSwap Algorithm

Algorithm 1

```

1: procedure NODESWAP( $\theta$ ) ▷ Input current iterate  $\theta$ 
2:    $\theta' \leftarrow \theta$ 
3:    $l \sim Unif(n)$  ▷ Sample random layer
4:    $i \sim Geom(\alpha^{-1})$  ▷ Sample random node
5:   while  $i \geq N_l$  do ▷ Repeat process until we have a valid node index
6:      $i \sim Geom(\alpha^{-1})$ 
7:   end while
8:    $w_{i+1,j}^{(l)'} \leftarrow w_{i,j}^{(l)}$ 
9:    $w_{i,j}^{(l)'} \leftarrow w_{i+1,j}^{(l)}$ 
10:   $w_{i,j+1}^{(l+1)'} \leftarrow w_{i,j}^{(l+1)}$ 
11:   $w_{i,j}^{(l+1)'} \leftarrow w_{i,j+1}^{(l+1)}$ 
12:   $b_{i+1}^{(l)'} \leftarrow b_i^{(l)}$ 
13:   $b_i^{(l)'} \leftarrow b_{i+1}^{(l)}$ 
14:   $u \sim Unif([0, 1])$ 
15:   $a = \min(1, \mu_0(\theta')/\mu_0(\theta))$  ▷ Metropolis-Hastings acceptance probability cf. (62)
16:  if  $u < a$  then
17:    return  $\theta'$  ▷ Accept node swap
18:  else
19:    return  $\theta$  ▷ Reject node swap
20:  end if
21: end procedure

```

B Proofs

Before turning to the proofs of the lemmas and theorems from the main paper, consider the n -layer fully connected feed-forward neural network in (11). When the layers have infinite width, we delineate the domain of the sequences that define each layer separately. For layer $1 < l < n + 1$ let

$$\mathcal{H}_w^{(l)} = \left\{ (w_{i,j}^{(l)})_{i,j \in \mathbb{N}} : \sum_{i=1}^{\infty} \sum_{j=1}^{\infty} (w_{i,j}^{(l)})^2 < \infty \right\}, \quad \mathcal{H}_b^{(l)} = \left\{ (b_i^{(l)})_{i \in \mathbb{N}} : \sum_{i=1}^{\infty} (b_i^{(l)})^2 < \infty \right\}. \quad (30)$$

(We omit the obvious modification for the sequence spaces for layer 1 and $n + 1$.) The entire network is then parameterised by

$$\mathcal{H} = \mathcal{H}^{(1)} \times \dots \times \mathcal{H}^{(n+1)}, \quad \text{where } \mathcal{H}^{(l)} = \mathcal{H}_w^{(l)} \times \mathcal{H}_b^{(l)}. \quad (31)$$

This domain is chosen because it has full measure under our Hilbert space Gaussian prior and also results in the infinite width functions in (13) being well defined almost surely.

B.1 Lemma 2

Lemma 2. *Consider the n -layer fully connected feed-forward neural network in (11). When the layers have infinite width, their weights and biases can be equivalently parameterised by $\ell^2 = \{(a_1, a_2, \dots) \in \mathbb{R}^{\mathbb{N}} : \sum_i a_i^2 < \infty\}$.*

Proof. $\mathcal{H}_w^{(l)}$ in (30) is an instance of the Hilbert space ℓ^2 since $\mathbb{N} \times \mathbb{N}$ is countable and any enumeration (e.g. the ‘diagonal’ enumeration method) of $\mathcal{H}_w^{(l)}$ to map its elements to infinite sequences of the form (a_1, a_2, \dots) will be square summable. Similarly, $\mathcal{H}_b^{(l)} = \mathcal{H}_w^{(l)} \times \mathcal{H}_b^{(l)}$, the cartesian product of two ℓ^2 spaces is again an instance of ℓ^2 regardless of how the two sequences are merged into one. Finally, by the same arguments, $\mathcal{H} = \mathcal{H}^{(1)} \times \dots \times \mathcal{H}^{(n+1)}$ is also an instance of ℓ^2 . \square

B.2 Proof of Theorem 1

Proof of Theorem 1. We prove the claims in the theorem for the infinite width case and in doing so cover the finite width case; the finite-dimensional case follows by omitting the limit arguments.

Lemma 2 shows that the weights and biases of the infinite width and finite depth neural network can be equivalently parameterised by ℓ^2 . As the biases and weights of each layer are independent zero mean Gaussian random variables, and the variances form a summable sequence when $\alpha > 1$, the prior μ_0 is a trace-class Gaussian prior on ℓ^2 and thus Property 1 is satisfied.

To see Property 6, by looking at the first layer we can easily check that for fixed $x \in [0, 1]^d$, $f_i^{(1)}(x)$ is a mixture of centered Gaussian distributions, and the claim follows by noting that $\mathbb{E}B_i^{(1)} = \mathbb{E}W_{i,j}^{(1)} = 0$,

$$\begin{aligned} \mathbb{E} \left[(f_i^{(1)}(x))^2 \right] &= \mathbb{E} \left[(B_i^{(1)})^2 \right] + \sum_{j=1}^d \mathbb{E} \left[(W_{i,j}^{(1)})^2 \right] (x_j)^2 \\ &\leq \frac{\sigma_{b_1}^2}{i^\alpha} + \frac{\sigma_{w_1}^2}{i^\alpha} d \end{aligned} \quad (32)$$

$$= \frac{1}{i^\alpha} [\sigma_{b_1}^2 + \sigma_{w_1}^2 d]. \quad (33)$$

We use induction over l , and define the following random variables, for which we truncate the i -th function of layer l after k terms:

$$f_{i,k}^{(l)}(x) = B_i^{(l)} + \sum_{j=1}^k W_{i,j}^{(l)} \zeta(F_j^{(l-1)}(x)) \quad l = 2 \dots n+1.$$

(Note that, with slight abuse of notation, we write $F_j^{(1)}$ even for the functions on the first layer, which are defined by finitely many parameters.)

It will be useful to note that by Assumption 9 and the induction hypothesis, we get

$$|\zeta(F_j^{(l-1)}(x))| \leq |(F_j^{(l-1)}(x))| < \infty. \quad (34)$$

Furthermore, from the above and using Jensen's inequality, we also obtain

$$|\mathbb{E}\zeta(F_j^{(l-1)}(x))| \leq \mathbb{E}|\zeta(F_j^{(l-1)}(x))| \leq \mathbb{E}|F_j^{(l-1)}(x)| < \infty, \quad (35)$$

where the last inequality holds as $F_j^{(l-1)}(x)$ is L^2 bounded by the induction hypothesis.

We now show that $f_{i,k}^{(l)}(x) \rightarrow F_i^{(l)}(x)$ almost surely, and in L^2 , by applying the L^2 martingale convergence theorem.

We thus need to show that $S_k(x) := f_{i,k}^{(l)}(x)$ is a L^2 bounded martingale, where we dropped the indices i and l for notational convenience. Indeed, with the natural filtration $(\mathcal{F}_k)_{k \in \mathbb{N}}$

$$\mathbb{E}[S_{k+1}(x)|\mathcal{F}_k] = 0,$$

as $W_{i,j}^{(l)}$ and $\zeta(F_j^{(l-1)}(x))$ are independent, the expectation of the former is centered, and the latter is finite. Additionally, by exploiting the independence, Assumption 9 and 35, we get

$$\mathbb{E} \left[(S_k(x))^2 \right] = \mathbb{E}[B_i^{(l)}]^2 + \sum_{j=1}^k \mathbb{E} \left[(W_{i,j}^{(l)})^2 \right] \mathbb{E} \left[(\zeta(F_j^{(l-1)}(x)))^2 \right] \quad (36)$$

$$\begin{aligned} &\leq \frac{\sigma_{b^{(l)}}^2}{i^\alpha} + \sigma_{w^{(l)}}^2 \sum_{j=1}^k \frac{1}{(ij)^\alpha} \mathbb{E} \left[(F_j^{(l-1)}(x))^2 \right] \leq \frac{\sigma_{b^{(l)}}^2}{i^\alpha} + \frac{\sigma_{w^{(l)}}^2 \sigma_{l-1}^2}{i^\alpha} \sum_{j=1}^k \frac{1}{j^{2\alpha}} \\ &= \frac{1}{i^\alpha} \left[\sigma_{b^{(l)}}^2 + \sigma_{w^{(l)}}^2 \sigma_{l-1}^2 \sum_{j=1}^k \frac{1}{j^{2\alpha}} \right]. \end{aligned} \quad (37)$$

This series converges for $\alpha > 1$, and we define the limit for $i = 1$ as σ_l^2 . Thus, S_k is indeed a L^2 bounded martingale and trivially $\mathbb{E}F_i^{(l)} = 0$, proving Assumption 6.

We next show Property 7. For the first layer, we use independence to get

$$\begin{aligned} \mathbb{E} \left[(f_i^{(1)}(x) - f_i^{(1)}(y))^2 \right] &= \sum_{j=1}^d \mathbb{E} \left[(W_{i,j}^{(1)})^2 \right] (x_j - y_j)^2 \\ &= \frac{\sigma_{w_1}^2}{i^\alpha} \|x - y\|^2. \end{aligned} \quad (38)$$

For the subsequent layers, we again use induction over l . We define $S_k(x)$ as before and check that

$$\mathbb{E} [(S_k(x)S_k(y))^2] = \mathbb{E} [(B_i^{(l)})^2] + \sum_{j=1}^k \mathbb{E} [(W_{i,j}^{(l)})^2] \mathbb{E} [\zeta(F_j^{(l-1)}(x))\zeta(F_j^{(l-1)}(y))]. \quad (39)$$

Using the induction hypothesis, Assumption 9, (36) and (39) we get

$$\begin{aligned} \mathbb{E} [(S_k(x) - S_k(y))^2] &= \mathbb{E} [(S_k(x))^2] + \mathbb{E} [(S_k(y))^2] - 2\mathbb{E}[S_k(x)S_k(y)] \\ &= 2\mathbb{E} [(B_i^{(l)})^2] + \sum_{j=1}^k \mathbb{E} [(W_{i,j}^{(l)})^2] \left(\mathbb{E} [\zeta(F_j^{(l-1)}(x))^2] + \mathbb{E} [\zeta(F_j^{(l-1)}(y))^2] \right) - 2\mathbb{E}[S_k(x)S_k(y)] \\ &= \sigma_{w^{(l)}}^2 \sum_{j=1}^k \frac{1}{(ij)^\alpha} \mathbb{E} [(\zeta(F_j^{(l-1)}(x)) - \zeta(F_j^{(l-1)}(y)))^2] \\ &\leq \sigma_{w^{(l)}}^2 \sum_{j=1}^k \frac{1}{(ij)^\alpha} \mathbb{E} [(F_j^{(l-1)}(x) - F_j^{(l-1)}(y))^2] \\ &\leq \frac{\sigma_{w^{(l)}}^2 c_{l-1}}{i^\alpha} \|x - y\|^2 \sum_{j=1}^k \frac{1}{j^{2\alpha}} \end{aligned} \quad (40)$$

$$= \frac{1}{i^\alpha} \left[\sigma_{w^{(l)}}^2 c_{l-1} \sum_{j=1}^k \frac{1}{j^{2\alpha}} \right] \|x - y\|^2, \quad (41)$$

such that the claim follows upon defining $c_l = \sigma_{w^{(l)}}^2 c_{l-1} \sum_{j=1}^\infty 1/j^{2\alpha}$, and noting that by the Fatou's lemma

$$\begin{aligned} \mathbb{E} [(F_i^{(l)}(x) - F_i^{(l)}(y))^2] &= \mathbb{E} \left[\liminf_{k \rightarrow \infty} (S_k(x) - S_k(y))^2 \right] \\ &\leq \liminf_{k \rightarrow \infty} \mathbb{E} [(S_k(x) - S_k(y))^2] \\ &\leq \sup_k \frac{1}{i^\alpha} \left[\sigma_{w^{(l)}}^2 c_{l-1} \sum_{j=1}^k \frac{1}{j^{2\alpha}} \right] \|x - y\|^2 \\ &= c_l \|x - y\|^2. \end{aligned}$$

Lastly, the claim of Property 8 for the finite width case follows by noting that the derivative exists almost surely (since we only sum finitely many Gaussians, and the activation function is a.s. differentiable by Assumption 9), and Property 8 is thus only violated on a zero probability event, since $\sigma_{w^{(l)}}^2 > 0$ for each l by assumption. \square

B.3 Lemma 3

In networks with small widths, Algorithm 1 gave acceptance rates of around 30% (for $N^{(l)} = 10$), which quickly declined as we included more nodes (e.g. 1% acceptances for $N^{(l)} = 100$.) This suggests that the NodeSwap algorithm is not well-defined in the infinite width limit, and this is indeed the statement of the next lemma. We will from now on write fraktal letters for the swapped nodes $f_i^{(l)}$ and $f_{i+1}^{(l)}$, and reserve i and l for general indices.

Lemma 3. *The NodeSwap Algorithm 1 which swaps the biases and weights associated with the nodes $f_i^{(l)}$ and $f_{i+1}^{(l)}$ is not well defined in the infinite width limit.*

For the finite width network, the acceptance ratio is given by

$$a^N(\theta^N, \vartheta^N) = \frac{\mu_0^N(\vartheta^N)}{\mu_0^N(\theta^N)}. \quad (42)$$

Proof. By Tierney et al. [1998], one needs to check that the measures $\eta(d\theta, d\vartheta) := \mu(\theta)Q(\theta, d\vartheta)$ and $\eta^T(d\theta, d\vartheta) := \eta(d\vartheta, d\theta) = \mu(d\vartheta)Q(\vartheta, d\theta)$ are mutually absolutely continuous on a set $R \in (E \times E, \mathcal{E} \otimes \mathcal{E})$, and mutually singular on R^C , where here Q is the deterministic transition kernel, and (E, \mathcal{E}) is the measurable space on which μ and Q are defined.⁶ The (deterministic) transition kernel Q maps θ to ϑ by swapping the nodes $f_{ij}^{(l)}$ and $f_{i(j+1)}^{(l)}$ (or more precisely,

⁶We use a different notation to Tierney et al. [1998]: Our η is his μ , our $m\mu$ is his π , our (θ, ϑ) is his (x, y) .

their associated weights and biases) with probability

$$\frac{1}{n} \times \frac{1}{i^\alpha} \frac{1}{\sum_{j=1}^{N^l} \frac{1}{j^\alpha}}, \quad (43)$$

which is well defined as $N^l \rightarrow \infty$, and independent of θ , such that it suffices to show that the measures $\mu(\theta)$ and $\mu^T(\theta) = \mu(\vartheta)$ are mutually absolutely continuous on a set $R_1 \in (E, \mathcal{E})$, and mutually singular on R_1^C . The likelihood is also invariant under the transformation $\theta \mapsto \vartheta$, and as it is integrable with respect to the prior by the assumptions in Section 2.2 [Stuart, 2010], we only need to show that the Gaussian measures $\mu_0(d\theta)$ and $\mu_0^T(d\theta)$ are absolutely continuous with respect to one another. Note that we can write these as

$$\mu_0(d\theta) = \mathcal{N}(0, \mathcal{C}) \quad (44)$$

$$\mu_0^T(d\theta) = \mathcal{N}(0, \tilde{\mathcal{C}}), \quad (45)$$

with diagonal (by assumption) covariance operators \mathcal{C} and $\tilde{\mathcal{C}}$, where the latter arises from swapping the variances associated with the swapped nodes. To see what is going on exactly, we now change to the neural network notation, where the variances under \mathcal{C} for the individual weights and biases were given by

$$W_{i,j}^{(1)} \sim \mathcal{N}\left(0, \frac{\sigma_{w^{(1)}}^2}{i^\alpha}\right), \quad W_{i,j}^{(l)} \sim \mathcal{N}\left(0, \frac{\sigma_{w^{(l)}}^2}{(ij)^\alpha}\right) \text{ for } l = 2 \dots n+1, \quad B_i^{(l)} \sim \mathcal{N}\left(0, \frac{\sigma_{b^{(l)}}^2}{i^\alpha}\right). \quad (46)$$

The variances under $\tilde{\mathcal{C}}$ are the same for most weights and biases, changed are only those associated with the swap nodes (recall that we swap nodes $f_{ij}^{(l)}$ and $f_{i(j+1)}^{(l)}$). The only changed variances are

$$W_{i,j}^{(l)} \sim \mathcal{N}\left(0, \frac{\sigma_{w^{(l)}}^2}{((i+1)j)^\alpha}\right), \quad W_{(i+1),j}^{(l)} \sim \mathcal{N}\left(0, \frac{\sigma_{w^{(l)}}^2}{(ij)^\alpha}\right), \quad \forall j \in \mathbb{N} \quad (47)$$

$$W_{i,j}^{(l+1)} \sim \mathcal{N}\left(0, \frac{\sigma_{w^{(l+1)}}^2}{(i(j+1))^\alpha}\right), \quad W_{i(j+1)}^{(l+1)} \sim \mathcal{N}\left(0, \frac{\sigma_{w^{(l+1)}}^2}{(ij)^\alpha}\right), \quad \forall i \in \mathbb{N} \quad (48)$$

$$B_i^{(l)} \sim \mathcal{N}\left(0, \frac{\sigma_{b^{(l)}}^2}{(i+1)^\alpha}\right) \quad B_{i+1}^{(l)} \sim \mathcal{N}\left(0, \frac{\sigma_{b^{(l)}}^2}{i^\alpha}\right), \quad (49)$$

which corresponds to swapping all the weights going into the nodes, swapping all the weights leaving the nodes, and swapping the biases of the nodes, respectively (see Figure 2 for an illustration).

We apply the Feldman-Hajek Theorem [Da Prato and Zabczyk, 2014, Theorem 2.25] to prove that these two Gaussian measures are mutually singular, by showing that the operator $(\mathcal{C}^{-1/2}\tilde{\mathcal{C}}^{1/2})(\mathcal{C}^{-1/2}\tilde{\mathcal{C}}^{1/2})^*$ is *not* a Hilbert-Schmidt operator. Due to the diagonality of \mathcal{C} and $\tilde{\mathcal{C}}$ the operator would be a Hilbert-Schmidt operator if

$$\sum_{i=1}^{\infty} \left(\frac{\tilde{\lambda}_i^2}{\lambda_i^2} - 1 \right)^2 < \infty. \quad (50)$$

We only need to check those terms where $\tilde{\lambda}_i \neq \lambda_i$. Again looking at only the eigenvalues corresponding to the weights going into the swapped nodes, and switching to the neural network parametrisation, we have

$$\sum_{j=1}^{\infty} \left(\frac{(ij)^\alpha}{((i+1)j)^\alpha} - 1 \right)^2 + \sum_{j=1}^{\infty} \left(\frac{((i+1)j)^\alpha}{(ij)^\alpha} - 1 \right)^2 = \infty, \quad (51)$$

such that the operator is *not* a Hilbert-Schmidt operator, and the Gaussian measures are mutually singular.

For the interested reader, note that the other two conditions of the Feldman-Hajek Theorem [Da Prato and Zabczyk, 2014, Theorem 2.25] are satisfied. First we show only that there exist constants L and U such that for any $\theta \in \ell^2$,

$$L|\tilde{\mathcal{C}}\theta| \leq |\mathcal{C}\theta| \leq U|\tilde{\mathcal{C}}\theta|, \quad (52)$$

which is equivalent to

$$L \sum_{i=1}^{\infty} (\theta_i \tilde{\lambda}_i^2)^2 \leq \sum_{i=1}^{\infty} (\theta_i \lambda_i^2)^2 \leq U \sum_{i=1}^{\infty} (\theta_i \tilde{\lambda}_i^2)^2, \quad (53)$$

where λ_i^2 are the respective variances corresponding to the values. Firstly note that we only need to consider those terms for which $\tilde{\lambda}_i^2 \neq \lambda_i^2$. Using the neural network parametrisation, we can split the problem in showing that (53) holds for

A) all the weights going into the swapped nodes, B) all the weights leaving the swapped nodes, and C) swapping the biases. Looking at the weights going into the swapped nodes, note that

$$\sum_{j=1}^{\infty} \left(\frac{w_{ij}^{(l)}}{((i+1)j)^{\alpha}} \right)^2 + \sum_{j=1}^{\infty} \left(\frac{w_{(i+1)j}^{(l)}}{(ij)^{\alpha}} \right)^2 = \sum_{j=1}^{\infty} \left(\frac{w_{ij}^{(l)}}{(ij)^{\alpha}} \right)^2 \left(\frac{(ij)^{\alpha}}{((i+1)j)^{\alpha}} \right)^2 + \sum_{j=1}^{\infty} \left(\frac{w_{(i+1)j}^{(l)}}{((i+1)j)^{\alpha}} \right)^2 \left(\frac{((i+1)j)^{\alpha}}{(ij)^{\alpha}} \right)^2 \quad (54)$$

$$\leq \sum_{j=1}^{\infty} \left(\frac{w_{ij}^{(l)}}{(ij)^{\alpha}} \right)^2 + 2^{2\alpha} \sum_{j=1}^{\infty} \left(\frac{w_{(i+1)j}^{(l)}}{((i+1)j)^{\alpha}} \right)^2 \quad (55)$$

$$\leq 2^{2\alpha} \left[\sum_{j=1}^{\infty} \left(\frac{w_{ij}^{(l)}}{(ij)^{\alpha}} \right)^2 + \sum_{j=1}^{\infty} \left(\frac{w_{(i+1)j}^{(l)}}{((i+1)j)^{\alpha}} \right)^2 \right], \quad (56)$$

and

$$\sum_{j=1}^{\infty} \left(\frac{w_{ij}^{(l)}}{(ij)^{\alpha}} \right)^2 + \sum_{j=1}^{\infty} \left(\frac{w_{(i+1)j}^{(l)}}{((i+1)j)^{\alpha}} \right)^2 = \sum_{j=1}^{\infty} \left(\frac{w_{ij}^{(l)}}{((i+1)j)^{\alpha}} \right)^2 \left(\frac{((i+1)j)^{\alpha}}{(ij)^{\alpha}} \right)^2 + \sum_{j=1}^{\infty} \left(\frac{w_{(i+1)j}^{(l)}}{(ij)^{\alpha}} \right)^2 \left(\frac{(ij)^{\alpha}}{((i+1)j)^{\alpha}} \right)^2 \quad (57)$$

$$\leq 2^{2\alpha} \sum_{j=1}^{\infty} \left(\frac{w_{ij}^{(l)}}{((i+1)j)^{\alpha}} \right)^2 + \sum_{j=1}^{\infty} \left(\frac{w_{(i+1)j}^{(l)}}{(ij)^{\alpha}} \right)^2 \quad (58)$$

$$\leq 2^{2\alpha} \left[\sum_{j=1}^{\infty} \left(\frac{w_{ij}^{(l)}}{((i+1)j)^{\alpha}} \right)^2 + \sum_{j=1}^{\infty} \left(\frac{w_{(i+1)j}^{(l)}}{(ij)^{\alpha}} \right)^2 \right] \quad (59)$$

such that for the weights going into the swapped nodes, (53) holds with $L = 2^{-2\alpha}$ and $U = 2^{2\alpha}$. Repeating the same argument for the weights leaving the swapped nodes and for the biases, shows that (53) holds in general with $L = 2^{-2\alpha}$ and $U = 2^{2\alpha}$. The remaining condition of the Feldman-Hajek theorem addresses the difference of means, but as $\theta = 0$ this is clearly in the Cameron-Martin space of the prior.

For the acceptance ratio in the finite width networks, observe that the likelihood does not depend on the labelling of the nodes and thus plays no role in the acceptance probability. Similarly, the transition kernel is symmetric, as nodes $f_i^{(l)}$ and $f_{i+1}^{(l)}$ are swapped with probability

$$q^N(\vartheta^N | \theta^N) = \mathbb{P}(\{\text{layer } l \text{ gets chosen}\}) \times \mathbb{P}(\{\text{node } i \text{ gets chosen}\} | \{\text{layer } l \text{ got chosen}\}) \quad (60)$$

$$= \frac{1}{n+1} \times \frac{1}{i^{\alpha}} \frac{1}{\sum_{j=1}^{N^l} \frac{1}{j^{\alpha}}}. \quad (61)$$

For the finite dimensional case we thus get

$$a^N(\theta^N, \vartheta^N) = \frac{\mu_0^N(\vartheta^N)}{\mu_0^N(\theta^N)} \frac{\mathcal{L}^N(\vartheta^N)}{\mathcal{L}^N(\theta^N)} \frac{q^N(\theta^N | \vartheta^N)}{q^N(\vartheta^N | \theta^N)} = \frac{\mu_0^N(\vartheta^N)}{\mu_0^N(\theta^N)}, \quad (62)$$

which is as required. \square

B.4 Proof of Theorem 2

Proof of Theorem 2. In the following, we identify v with its finitely many observations v_t . One notes that the integral (20) is upper bounded by 1. For the lower bound we substitute $w = u - v$ in (20), allowing us to bound

$$\begin{aligned}
(20) &= \int \mathbb{1}_{\{u \in \mathbb{R}^d : (w+v)_1 \geq (w+v)_j \forall j \neq 1\}} \mathcal{N}(w; 0, \sigma^2 I_{M \times M}) dw \\
&\geq \int \mathbb{1}_{\{w \in \mathbb{R}^d : (w+v)_1 \geq 0 \geq (w+v)_j \forall j \neq 1\}} \mathcal{N}(w; 0, \sigma^2 I_{M \times M}) dw \\
&= \int \mathbb{1}_{\{w \in \mathbb{R}^d : w_1 \geq -v_1, w_j \leq -v_j \forall j \neq 1\}} \mathcal{N}(w; 0, \sigma^2 I_{M \times M}) dw \\
&= \int \mathbb{1}_{\{w \in \mathbb{R}^d : w_1 \geq -v_1, w_j \geq v_j \forall j \neq 1\}} \mathcal{N}(w; 0, \sigma^2 I_{M \times M}) dw \tag{63}
\end{aligned}$$

$$\begin{aligned}
&\geq \int \mathbb{1}_{\{w \in \mathbb{R}^d : w_1 \geq |-v_1|, w_j \geq |v_j| \forall j \neq 1\}} \mathcal{N}(w; 0, \sigma^2 I_{M \times M}) dw \\
&\geq \int \mathbb{1}_{\{w \in \mathbb{R}^d : w_1 \geq s, w_j \geq s \forall j \neq 1\}} \mathcal{N}(w; 0, \sigma^2 I_{M \times M}) dw, \tag{64}
\end{aligned}$$

where for (63) we exploited the fact that the normal is centered and isotropic, and to get (64) we pick $s = \|v\|_\infty > 0$ if $v \neq 0$. The case $v = 0$ is trivial as the integral is then non-zero. (64) can now be treated as the tail probability for a centered multivariate normal distribution (see Hashorva [2005]) which satisfies the Savage condition Savage [1962]. We thus get the bound

$$(64) \geq c \exp(-s^2) = c \exp(-\|v\|_\infty^2)$$

as long as $\|v\|_\infty > 2d/\sigma^4$. For all other v , the integral (20) is bounded away from zero, and the Assumption 3 holds trivially. The assumption thus holds for all v .

To see that Assumption 4 holds, note that the log-likelihood is continuously differentiable in v , and thus locally Lipschitz. \square

B.5 Proof of Theorem 3

Proof of Theorem 3. Firstly, note that the Assumptions in Theorem 1 hold by Theorem 2, and additionally the log-likelihood ℓ satisfies $\sum_{k=1}^M \frac{\partial \ell}{\partial v_k} = 0$ (where v_k is the evaluation $v(x_k)$ of the value function at location x_k) by the translation invariance, and $\sum_{k=1}^M \left(\frac{\partial \ell}{\partial v_k} \right)^2 < \infty$ for any v μ_0 -almost surely.

For the KL prior, the claim follows immediately from the Feldman-Hajek theorem (see e.g. Da Prato and Zabczyk [2014])

For simplicity, we from now on assume that the likelihood consists of only one data point and omit the respective index, but the generalisation to multiple data points is trivial.

Following a similar argument as in the proof of Theorem 1, we will show that for fixed x

$$S_s = S_s(x) = \sum_{l=1}^{n+1} \sum_{i=1}^s \left[\frac{\sigma_{b_l}^2}{i^\alpha} \left(\frac{\partial \ell}{\partial B_i^{(l)}}(x) \right)^2 + \sum_{j=1}^s \frac{\sigma_{w_l}^2}{(ij)^\alpha} \left(\frac{\partial \ell}{\partial W_{i,j}^{(l)}}(x) \right)^2 \right] \tag{65}$$

defines a L^1 -bounded submartingale, converging almost surely to a random variable S_∞ by Doob's martingale convergence theorem. Once we have established the convergence, we note that this implies the equivalence

$$\mathcal{N}(\mathcal{CD}\ell(u), \mathcal{C}) \simeq \mathcal{N}(0, \mathcal{C}) \tag{66}$$

for all u π_0 -almost surely by applying (a simplified version of) the Feldman-Hajek theorem [Da Prato and Zabczyk, 2014, Theorem 2.23] which states that two Gaussian measures $\mathcal{N}(m_1, Q)$ and $\mathcal{N}(m_2, Q)$ are absolutely continuous with respect to one another if and only if $m_1 - m_2 \in Q^{1/2}(\mathcal{H})$, i.e. $\sum_i (m_{1i} - m_{2i})^2 / \lambda_i^2 < \infty$ [Da Prato and Zabczyk, 2014]⁷. Here, the latter corresponds to

$$\sum_{i=1}^{\infty} \frac{(\mathcal{CD}\ell(u))_i^2}{\lambda_i^2} = \sum_{i=1}^{\infty} \frac{\lambda_i^4 (\mathcal{D}\ell(u))_i^2}{\lambda_i^2} = \sum_{i=1}^{\infty} \lambda_i^2 (\mathcal{D}\ell(u))_i^2 \tag{67}$$

⁷In our notation, the eigenvalues of \mathcal{C} are λ_i^2 , in comparison to the ones used in Da Prato and Zabczyk [2014] who define the eigenvalues of \mathcal{Q} as λ .

being finite [Da Prato and Zabczyk, 2014]. Note that $\mathcal{D}\ell(u)$ is a random variable defined over the parameters of the neural network; Equation 67 is, after substituting both the eigenvalues of \mathcal{C} and the derivatives with respect to the parameters into this expression, equivalent to Equation 65. We will show that S_s is finite π_0 -almost surely such that the equivalence (66) holds.

Remark: We here also note that, if we want to apply the same argument for the case without preconditioning, we would require (by the same argument as above) that

$$\sum_{i=1}^{\infty} \frac{(\mathcal{D}\ell(u))_i^2}{\lambda_i^2} = \sum_{i=1}^{\infty} \frac{(\mathcal{D}\ell(u))_i^2}{\lambda_i^2} < \infty,$$

which will generally not be the case. One can check this by repeating the proof for the pCNL case (note that the likelihood contribution would have to dominate the diverging $1/\lambda_i^2$ terms).

It remains to show that S_s is a L^1 -bounded submartingale. It is clear that S_s is a (non-negative) submartingale, and we only need to show that the expectation of S_s is bounded. We define $g_i^{(l)}(x) = \varphi(f_i^{(l)}(x))$ to simplify notation. From (37) we get $\mathbb{E}[(f_i^{(l)})^2] \leq \sigma_l^2/i^\alpha$, and combining this bound with Assumption 9, we get $\mathbb{E}[(g_i^{(l)})^2] \leq \sigma_l^2/i^\alpha$. We ask the reader to recall Definition 11. The partial derivatives with respect to the biases and weights can be calculated by applying the chain rule multiple times, and they are given by

$$\frac{\partial \ell}{\partial W_{1,j}^{(n+1)}} = \sum_{k=1}^M \frac{\partial v_k}{\partial W_{1,j}^{(n+1)}} \frac{\partial \ell}{\partial v_k} = \sum_{k=1}^M g_{1,j}^{(n)}(x^k) \frac{\partial \ell}{\partial v_k} \quad (68)$$

$$\frac{\partial \ell}{\partial B_1^{(n+1)}} = \sum_{k=1}^M \frac{\partial v_k}{\partial B_1^{(n+1)}} \frac{\partial \ell}{\partial v_k} = \sum_{k=1}^M \frac{\partial \ell}{\partial v_k} \quad (69)$$

$$\frac{\partial \ell}{\partial W_{i,j}^{(l)}} = \frac{\partial f_i^{(l)}}{\partial W_{i,j}^{(l)}} \frac{\partial \ell}{\partial f_i^{(l)}} = g_j^{(l-1)} \frac{\partial \ell}{\partial f_i^{(l)}} \quad l = 2 \dots n \quad (70)$$

$$\frac{\partial \ell}{\partial B_i^{(l)}} = \frac{\partial f_i^{(l)}}{\partial B_i^{(l)}} \frac{\partial \ell}{\partial f_i^{(l)}} = \frac{\partial \ell}{\partial f_i^{(l)}} \quad l = 2 \dots n \quad (71)$$

$$\frac{\partial \ell}{\partial W_{i,j}^{(1)}} = x_j \frac{\partial \ell}{\partial f_i^{(1)}} \quad (72)$$

$$\frac{\partial \ell}{\partial B_i^{(1)}} = \frac{\partial \ell}{\partial f_i^{(1)}}. \quad (73)$$

We will have to consider the following partial derivatives that show up in the ones above:

$$\frac{\partial \ell}{\partial f_i^{(l)}(x)} = \frac{\partial g_i^{(l)}(x)}{\partial f_i^{(l)}(x)} \frac{\partial \ell}{\partial g_i^{(l)}(x)} \quad l = 1 \dots n \quad (74)$$

$$\frac{\partial \ell}{\partial g_i^{(l)}(x)} = \sum_{j=1}^s \frac{\partial \ell}{\partial f_j^{(l+1)}(x)} W_{j,i}^{(l+1)} \quad l = 1 \dots n, \quad (75)$$

where in the last line we have already established the dependence of $\frac{\partial \ell}{\partial g_i^{(l)}(x)}$ on s . Using Assumption 9, we get that

$$\left| \frac{\partial g_i^{(l)}}{\partial f_i^{(l)}} \right| \leq 1.$$

Now, for $l = n$, by independence:

$$\mathbb{E} \left[\left(\frac{\partial \ell}{\partial g_i^{(l)}} \right)^2 \right] = \mathbb{E} \left[\left(\frac{\partial \ell}{\partial f_1^{(n+1)}} W_{1,i}^{(n+1)} \right)^2 \right] \quad (76)$$

$$= \frac{\sigma_{w_{n+1}}^2}{i^\alpha} \sum_{k=1}^M \left(\frac{\partial \ell}{\partial v_k} \right)^2, \quad (77)$$

and further (again by independence), for $l < n$,

$$\mathbb{E} \left[\left(\frac{\partial \ell}{\partial g_i^{(l)}} \right)^2 \right] = \sum_{j=1}^s \mathbb{E} \left[\left(\frac{\partial \ell}{\partial f_j^{(l+1)}} W_{j,i}^{(l+1)} \right)^2 \right] \quad (78)$$

$$= \frac{\sigma_{w_{l+1}}^2}{i^\alpha} \sum_{j=1}^s \frac{1}{j^\alpha} \mathbb{E} \left[\left(\frac{\partial \ell}{\partial f_j^{(l+1)}} \right)^2 \right] \quad (79)$$

$$= \frac{\sigma_{w_{l+1}}^2}{i^\alpha} \sum_{j=1}^s \frac{1}{j^\alpha} \mathbb{E} \left[\left(\frac{\partial g_j^{(l+1)}}{\partial f_j^{(l+1)}} \frac{\partial \ell}{\partial g_j^{(l+1)}} \right)^2 \right] \quad (80)$$

$$\leq \frac{\sigma_{w_{l+1}}^2}{i^\alpha} \sum_{j=1}^s \frac{1}{j^\alpha} \mathbb{E} \left[\left(\frac{\partial \ell}{\partial g_j^{(l+1)}} \right)^2 \right]. \quad (81)$$

We can use induction to show that for $l = 1 \dots n$,

$$\mathbb{E} \left[\left(\frac{\partial \ell}{\partial g_i^{(l)}} \right)^2 \right] \leq \frac{d_l}{i^\alpha} \sum_{k=1}^M \left(\frac{\partial \ell}{\partial v_k} \right)^2, \quad (82)$$

where

$$d_l = \left(\prod_{r=l+1}^{n+1} \sigma_{w_r}^2 \right) \left(\sum_{j=1}^{\infty} 1/j^{2\alpha} \right)^{n+1-l-1}. \quad (83)$$

Putting things together, we get that (65) defines a L^1 bounded submartingale if $\alpha > 1$ and $\sum_{k=1}^M \left(\frac{\partial \ell}{\partial v_k} \right)^2 < \infty$:

$$\begin{aligned} \mathbb{E}[S_s] &= \mathbb{E} \left[\sum_{l=1}^{n+1} \sum_{i=1}^s \left[\frac{\sigma_{b_l}^2}{i^\alpha} \left(\frac{\partial \ell}{\partial B_i^{(l)}}(x) \right)^2 + \sum_{j=1}^s \frac{\sigma_{w_l}^2}{(ij)^\alpha} \left(\frac{\partial \ell}{\partial W_{i,j}^{(l)}}(x) \right)^2 \right] \right] \\ &\leq \max_l [\max(\sigma_{b_l}^2, \sigma_{w_l}^2)] \mathbb{E} \left[\sum_{l=1}^{n+1} \sum_{i=1}^s \left[\left(\frac{\partial \ell}{\partial B_i^{(l)}}(x) \right)^2 + \sum_{j=1}^s \left(\frac{\partial \ell}{\partial W_{i,j}^{(l)}}(x) \right)^2 \right] \right], \end{aligned}$$

and it remains to show that the expectation part of this expression is finite:

$$\begin{aligned} &E \sum_{l=1}^{n+1} \sum_{i=1}^s \left[\left(\frac{\partial \ell}{\partial B_i^{(l)}}(x) \right)^2 + \sum_{j=1}^s \left(\frac{\partial \ell}{\partial W_{i,j}^{(l)}}(x) \right)^2 \right] \\ &= \mathbb{E} \sum_{l=1}^{n+1} \sum_{i=1}^s \left[\left(\frac{\partial g_i^{(l)}}{\partial f_i^{(l)}} \frac{\partial \ell}{\partial g_i^{(l)}} \right)^2 + \sum_{j=1}^s \left(g_j^{(l-1)} \frac{\partial g_i^{(l)}}{\partial f_i^{(l)}} \frac{\partial \ell}{\partial g_i^{(l)}} \right)^2 \right] \\ &\leq \mathbb{E} \sum_{l=1}^{n+1} \sum_{i=1}^s \left[\left(\frac{\partial \ell}{\partial g_i^{(l)}} \right)^2 + \sum_{j=1}^s \left(g_j^{(l-1)} \frac{\partial \ell}{\partial g_i^{(l)}} \right)^2 \right] \\ &= \sum_{l=1}^{n+1} \sum_{i=1}^s \left[\mathbb{E} \left[\left(\frac{\partial \ell}{\partial g_i^{(l)}} \right)^2 \right] + \sum_{j=1}^s \mathbb{E} \left[\left(g_j^{(l-1)} \frac{\partial \ell}{\partial g_i^{(l)}} \right)^2 \right] \right] \\ &\leq \sum_{l=1}^{n+1} \sum_{i=1}^s \left[\frac{d_l}{i^\alpha} \sum_{k=1}^M \left(\frac{\partial \ell}{\partial v_k} \right)^2 + \frac{d_l}{i^\alpha} \sum_{k=1}^M \left(\frac{\partial \ell}{\partial v_k} \right)^2 \sum_{j=1}^s \frac{\sigma_l^2}{j^\alpha} \right] \\ &\leq \sum_{k=1}^M \left(\frac{\partial \ell}{\partial v_k} \right)^2 \sum_{l=1}^{n+1} d_l \sum_{i=1}^s \left[\frac{1}{i^\alpha} \left(1 + \sum_{j=1}^s \frac{\sigma_l^2}{j^\alpha} \right) \right] < \infty. \end{aligned}$$

□

B.6 Proof of pCNL being well-defined.

Theorem 4. *The preconditioned Crank-Nicolson Langevin algorithm is a well-defined MCMC algorithm in the function space setting if $\mathcal{CD}\Phi(u) \in \text{Im}(\mathcal{C}^{1/2})$.*

Part of this proof can be found in Beskos et al. [2017].

Proof. We assume that [Cotter et al., 2013, Theorem 6.2] holds. We can then check that the change of measure arising from the gradient term is absolutely continuous with respect to the measures used in Theorem 6.2 if, and only if, $\mathcal{CD}\Phi(u) \in \text{Im}(\mathcal{C}^{1/2})$ by the Cameron-Martin Theorem Cameron and Martin [1944]. \square

C Details on experimental setup

We here give further details on the experimental setup for the Examples 5.1. Both examples are included in the python package ‘gym’ [Brockman et al., 2016].

C.1 Mountaincar

The first example is the popular mountaincar problem. The state space is the 2-dimensional domain $\mathcal{X} = [-1.2, 0.6] \times [-0.07, 0.07]$, where the first variable is the position x_1 of the car on a mountain slope, and the second variable represents its velocity x_2 . The set of possible actions is $\mathcal{A} = \{-1, 0, 1\}$, representing exerting force to the left, not adding force, and exerting force to the right, respectively. The state transitions are deterministic, being given by Newtonian physics, and we refer the reader to the OpenAI documentation or to our code for the details.

In the mountaincar problem, the reward is constant $r(x_1, x_2) = -1$ per step, until the car reaches the top of the mountain ($x_1 \geq 0.5$). The optimal policy is therefore to reach the mountaintop as quickly as possible. An optimal deterministic policy [Xiao, 2019] is given by

$$\mu(x_1, x_2) = -1 + 2\mathbb{I}\{\min(-0.09(x_1 + 0.25)^2 + 0.03, 0.3(x_1 + 0.9)^4 - 0.008) \leq x_2 \leq -0.07(x_1 + 0.38)^2 + 0.07\},$$

and we generated state-action pairs by firstly drawing a random initial state in the valley of the mountain, $x \sim \mathcal{U}([-0.6, -0.4])$, i.e. a uniform value between -0.6 and -0.4 . The initial velocity is set to 0. Starting from that state, we computed the action given the optimal policy given above. Once the flag was reached, a new initial state was drawn, and the process repeated until we had a total of 250 observations. This gave a set of state-action pairs $\{(x_t, a_t)\}_{t=1}^{250}$, and we then took every fifth sample to obtain the final dataset $y = \{(x_{5t}, a_{5t})\}_{t=1}^{50}$. This resulted in the state variables in y covering the entire state space, such that we can expect to learn the value function in any region an agent might find themselves in. The likelihood (22) arises from this dataset y and the noise level being set to $\sigma = 0.1$.

In the simulations from the learned value functions, we again initialised the state variable as $x \sim \mathcal{U}([-0.6, -0.4])$ and set the velocity to 0. We then simulated noise and used Equation (18) with the learned value function to pick an action. In Section 5.3, the used value function was taken as either a sample from the posterior or as the mean function; in Section 5.4 the used value function was the mean function from the posteriors. In all experiments, if the car didn’t make it to the flag within 200 time steps, we called this a failure and restarted the process from new initial conditions.

C.2 HalfCheetah

To show that our algorithm works in a more complicated setting, we looked at the HalfCheetah example from the MuJoCo library [Todorov et al., 2012] where the state x_t a 17-dimensional vector. The original continuous actions space of the problem is 6-dimensional.

An agent controlling the cheetah is to move it to forward while not exerting too much force: positive rewards are given for moving forward, and negative rewards are given for moving backwards, a further penalty is deducted for actions requiring a lot of force. A black box optimal policy for the HalfCheetah problem was provided in Berkeley’s Deep Reinforcement Learning Course⁸, which we used to simulate state-action pairs.

The initial state and velocity variables were drawn at random with distributions according to the python package ‘gym’ [Brockman et al., 2016]. We discretised the action space to M actions in the following way: an initial state was drawn, and the black box policy gave us an action, taking us to a new state via deterministic mapping. Iterating this process, the first M actions were stored. From now on, we can use a discrete action space \mathcal{A}_M consisting of these M actions: at a state x_t we compute a_t as the action in \mathcal{A}_M that minimises the Euclidean distance to the action computed by the black box policy. We found that $M = 8$ actions were sufficient to get behaviour very similar to the one we got when using the continuous action space, and we thus fixed $\mathcal{A} = \mathcal{A}_8$. We refer to the action $a \in \mathcal{A}$ that minimises the Euclidean distance to the black box algorithm as ‘optimal’. To generate data, we firstly drew an initial state x_1 , and then computed the optimal action a_1 using the procedure just described, and computed the next state using the state dynamics (15). After 25 steps, we restarted from a new initial state, and repeated this process another 4 times until we had a total of $T = 100$ data points. The reason we restarted occasionally was, as in the mountaincar example, to ensure that we cover

⁸CS294-112 HW 1: Imitation Learning, <https://github.com/berkeleydeeprlcourse/homework/tree/master/hw1>

a representative region of the state space. The dataset $y = \{(x_t, a_t)\}_{t=1}^{100}$ was used in the likelihood (22), where we set the noise level to $\sigma = 0.1$. In the experiments in Section 5.4, an initial state is drawn, and the cheetah is controlled using Equation (18) over 100 time steps.